For Reference

NOT TO BE TAKEN FROM THIS ROOM

For Reference

NOT TO BE TAKEN FROM THIS ROOM

Ex libris
universitatis
albertaeensis

UNIVERSITY OF ALBERTA
QUAECUMQUE VERA

University of

Digitized by the Internet Archive
in 2018 with funding from
University of Alberta Libraries

https://archive.org/details/effectofrapidhea00hawo

esis
1964
#30

UNIVERSITY OF ALBERTA

# THE EFFECT OF RAPID HEATING ON THE ALPHA TO GAMMA TRANSFORMATION IN IRON

A THESIS
SUBMITTED TO THE FACULTY OF GRADUATE STUDIES
IN PARTIAL FULFILMENT OF THE REQUIREMENTS
FOR THE DEGREE OF MASTER OF SCIENCE

by

William Lancelot Haworth

DEPARTMENT OF MINING AND METALLURGY

EDMONTON

APRIL 1964

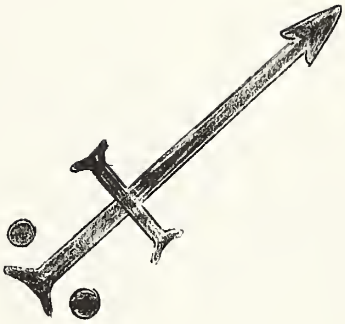

# ACKNOWLEDGEMENTS

I am glad to have this opportunity of thanking Dr. J. Gordon Parr for his guidance and unfailing encouragement, Dr. W. V. Youdelis for many helpful discussions, and my colleagues and friends in the Department for the advice, criticism and assistance without which a research project could never succeed. Thanks are also due to Dr. E. O. Lilge for his departmental supervision, and to Mr. Joel Mercier and Miss Aileen Cronin for their patience in deciphering my handwriting and typing the manuscript.

This work formed part of a project sponsored by the Defence Research Board of Canada.

# ABSTRACT

The effect of rapid heating on the $\alpha \longrightarrow \gamma$ transformation temperature in cold-worked and annealed Armco iron has been studied; the results are discussed in terms of the mode of carbon distribution in the iron, and the possible transformation mechanisms are critically assessed.

## CONTENTS

Page

1. INTRODUCTION AND REVIEW

The allotropy of iron. 1

The $\alpha \rightleftharpoons \gamma$ transformation. 2

The transformation mechanism. 3

2. EXPERIMENTAL PROCEDURE

Radiative heating. 9

Electrical heating (temperature measurement by photoelectric cell). 11

Electrical heating (temperature measurement by thermocouple). 13

The heating unit. 16

Recording the heating curve. 17

Preparation of specimens. 22

Checks on accuracy. 26

3. RESULTS

The transformation temperature. 29

The transformation time. 29

The latent heat of transformation. 29

Subsidiary results. 30

# CONTENTS

Page

4. DISCUSSION

The temperature measurement technique. 51

Treatment of data. 52

Interpretation of results. 54

Conclusions. 68

5. APPENDIX

Shear model for the transformation. 69

Measurement of parameters from the heating curve. 69

Correction of the transformation temperature. 72

Calculation of the latent heat. 72

6. BIBLIOGRAPHY

# LIST OF FIGURES

Page

2.1 Trial radiative heating unit (tantalum foil furnace). 10

2.2 Trial radiative heating unit (Fresnel lens system). 10

2.3 Balancing circuit (after Boedtker and Duwez). 15

2.4 Macrostructure of a thermocouple weld. 15

2.5 The heating and auxiliary circuits. 18

2.6 Schematic drawing of the heating unit. 20

2.7 Three typical heating curves. 21

2.8 ) ( cold-worked 24
) Representative (
2.9 ) ( annealed 600°C 24
) micro- (
2.10 ) ( annealed 800°C 25
) structures (
2.11 ) ( annealed 1000°C 25

3.1 Rate data, for cold-worked Armco iron. 32

3.2 Rate data, for Armco iron annealed at 600°C. 33

3.3 Rate data, for Armco iron annealed at 800°C. 34

3.4 Rate data, for Armco iron annealed at 1000°C 35

3.5 Rate data for cold-worked Armco iron held 1 minute at 800°C. 36

## LIST OF FIGURES (continued)

Page

3.6 Rate data for annealed (800°C) Armco iron held 1 minute at 800°C. 37

3.7 Rate data for annealed steel (logarithmic rate scale). 38

3.8 Data for cold-worked Armco iron heated from room temperature. 39

3.9 Data for cold-worked Armco iron heated from 800°C after 1 minute holding. 40

4.1 Part of the iron-carbon phase diagram (after Hansen). 58

4.2 Classification of phase transformations by diffusion lengths. 62

5.1(a) Shear model for the $\alpha \rightarrow \gamma$ transformation, single plane. 70

5.1(b) Shear model for the $\alpha \rightarrow \gamma$ transformation, (after Agarwala and Wilman). 70

5.2 Heating-curve parameters. 71

# LIST OF TABLES

Page

2.1 Iron analysis 23

2.2 Steel analysis 27

3.0 Heat treatments and key for tabulation of results. 41

3.1 Rate data for iron. 42

3.2 Rate data for iron. 43

3.3 Rate data for iron. 44

3.4 Rate data for iron. 45

3.5 Rate data for iron. 47

3.6 Rate data for iron. 48

3.7 Rate data for steel. 49

3.8 Radiative heating results. 50

4.1 (in text) Estimate of errors. 54

# 1. INTRODUCTION AND REVIEW

## 1.1 The Allotropy of Iron *

Metallurgical investigation of the allotropy of iron can be said to have begun almost a hundred years ago, with the discovery, by the Russian metallurgist Tschernoff, of the critical points in steel - although decalescence of steel on heating is mentioned as early as 1777. Subsequent research revealed the phenomenon of recalescence on cooling, and the existence of an anomalous specific heat in the neighbourhood of the critical points; in 1873 Tait demonstrated the allotropy of iron by measurements of thermal e.m.f., and further development of the thermocouple by Le Chatelier opened the way for thermal analysis. That there was a reasonable understanding of the nature of the transformation is shown by a statement of Sorby's concerning the recrystallization of iron on cooling from a high temperature:

> "... these facts make it extremely probable that a great molecular disturbance takes place in iron at a dull red heat similar to the change which occurs when yellow mercuric iodide formed at high temperatures turns red on cooling." (Sorby 1887)

---

* See Mehl, (1948), C.S. Smith (1960), Parr (1963) for detailed reviews and references to the original papers.

Osmond investigated the thermal arrests in iron and steel and concluded that iron exists in the allotropic forms alpha, beta and gamma, depending on temperature, and it is interesting to note that he was aware of the effects of cooling on the $\gamma \rightarrow \beta$ transformation. The relative roles of carbon and the allotropic transformation in the formation of "hardenite" (viz., martensite) were the source of much controversy in the closing years of the century.

With the development of X-ray analysis, the nature of the various allotropes of iron could be established; by 1922 Westgren and Phragmen had determined the crystal structures of alpha, beta, gamma and delta iron, finally laying the ghost of a structural transformation at the Curie point.

## 1.2 The $\alpha \rightleftharpoons \gamma$ Transformation

Several questions spring to mind at this point. The space-lattice of pure iron is body-centred cubic below about 910°C (alpha iron) and face-centred cubic (gamma iron) for several hundred degrees above 910°C; how, and why, does the transformation occur? Furthermore, what effect do alloying elements have on the transformation, and how is it affected by physical environment in the broadest sense?

Searching for the answers to such questions - with more or less success - has occupied metallurgists since the time of Tschernoff's

discovery, principally because the $\alpha \rightleftharpoons \gamma$ transformation in iron plays a vitally important part in determining the subsequent properties of steel. It has been the object of the present investigation to explore one facet of this many-sided problem, namely, the behaviour of the transformation under conditions of very rapid heating. In this way it might be possible to shed further light on the effect of rapid heating on the transformation temperature, time, and mechanism; the problem is not without practical interest, as recent investigations have shown that useful properties might be obtained by the rapid heating of iron and steel through the $A_3$ temperature during heat-treatment. (Kidin 1960 no. 1, Bodyako et al. 1960, Kuznetsov 1958.)

## 1.3 The Transformation Mechanism

Most phase transformations in metals can be placed in one of the following classifications, according to the mechanism by which they occur: *

(i) Processes involving long-range diffusion of atoms.

(ii) Diffusionless transformations.

(iii) Intermediate processes, which may involve short range diffusion.

Rapidly induced allotropic transformations in pure metals are usually placed in the second category, more on the basis of a consensus of opinion

---

* Buerger's suggestion that transformations may be 'reconstructive' or 'displacive', or a combination of both, is an intriguing restatement of the same idea. (Buerger 1951)

than on that of experimental evidence. In the case of iron, the relationship between temperature and the free energy difference between the alpha and gamma phases is known to arise from the difference in electronic specific heats of the two structures.* Zener (1955) has related this phenomenon to the gradual uncoupling of aligned spin magnetic moments of electrons in the d-shells of the iron atoms, as the temperature is raised above the Curie point. It is unlikely that such a process would require the diffusion of atoms through the crystal lattice, and so the $\alpha \longrightarrow \gamma$ transformation in pure iron can be placed confidently in the diffusionless category. The presence of small amounts of impurity may affect the free energy relationship considerably, however, by increasing the effect of the lattice contribution to the overall free energy.

Transformations involving a compositional change fall into the first category - although the arbitrary application of the classification to what is probably a "continuum" of mechanisms may inevitably cause confusion in borderline cases - since diffusion is necessary in order to create or develop nuclei of the new phase. Under certain conditions, long-range diffusion may give way to a process of the second or third type, and a different transformation product may result: a familiar example is the effect of cooling rate on the eutectoid reaction in steel, the product being pearlite, martensite, or

---

* Seitz 1940, Smoluchowski and Koehler 1941.

bainite according to whether the transformation occurs by a group (i), (ii) or (iii) mechanism.

The transformation occurring on heating hypo-eutectoid steel at various rates has been investigated by several Russian authors, whose work has been reviewed by Kidin (1957, 1960 no. 2.). He states that the temperature at which pearlite is completely converted into austenite may be as high as 1000°C at heating rates of several thousand degrees per second; it is also suggested that the hysteresis of the transformation temperature above the $A_3$ line is due to the time required for carbon to diffuse from the cementite plates into the neighbouring austenite.

Discussing the transformation of ferrite itself, Kidin suggests that austenite nuclei (whose critical size diminishes with increasing temperature) are created at temperatures as low as 820°C in cold-worked electrolytic iron, because of prior segregation of carbon to the boundaries of sub-grains or "mosaic blocks" in the ferrite. Such nuclei develop by a diffusion-controlled process until the A3 temperature of the interior of the mosaic blocks is reached; if the heating rate is sufficiently high this development may be relatively small, and the bulk of the ferrite then transforms into austenite by a diffusionless mechanism at the A3 temperature.

The process as a whole therefore defies definition in the usual way, although its parts are amenable to the classification outlined above.

It is interesting to note that Kidin's analysis is also applicable to the

transformation of free ferrite and the ferrite plates in hypo-eutectoid steel - austenite formed at rapid heating rates by the same mechanism will contain cementite, which subsequently dissolves by diffusion of carbon. However, it seems possible that the ferrite plates in pearlite might be transformed into austenite by a diffusion process (i.e. the growth of austenite nuclei formed at the ferrite-cementite interface) before the $A_3$ temperature of the ferrite is reached; Kidin calculated the critical rate required to reach the $A_3$ temperature before the diffusion-controlled transformation is completed, assuming a structure of coarse pearlite, and arrived at a figure in excess of 75,000°C per second.

Reference was made above to the postulate that a diffusionless mechanism is responsible for the bulk of the $\alpha \longrightarrow \gamma$ transformation in iron containing a small amount of carbon. Wilman and Agarwala (1953, 1954) proposed a crystallographic model for the transformation on the basis of their X-ray study of the relative orientations of alpha and gamma phases in iron, the gamma phase having been produced by abrading the surface of a single crystal of ferrite with fine emery paper. The model is described in part 5.1 of the appendix.

A study of the $\alpha \longrightarrow \gamma$ transformation in high-purity iron, containing 66 p.p.m. carbon, subjected to heating rates in the range 100°C per second to 7000°C per second (approximately) has recently been made by Boedtker and Duwez (1962). Their results show that the transformation

temperature is rate-dependent, and they relate the extent of this dependence to the activation energies for diffusion of carbon and nitrogen in ferrite, concluding that one or both of these interstitial elements influences the kinetics of the transformation. Their heating curves were obtained, however, from an initial holding temperature of 840°C, and it seems significant that at this temperature and carbon content, Kidin's model of segregation to mosaic boundaries producing austenite nuclei is probably no longer applicable.

Svechnikov et al (1955) report that there is no rate-dependence of the transformation temperature in steel in the range 20°C per second to 200°C per second, although the transformation temperature varies according to the initial microstructure. They conclude that the time required for completion of the transformation of a given structure into austenite, at the heating rates quoted, depends only on the rate of supply of heat to the specimen; however, no hypothesis as to the transformation mechanism or mechanisms is presented. A later paper (1959) by the same authors reports an investigation of the $\alpha \rightarrow \gamma$ transformation in Armco iron at a heating rate of about 900°C per second using dilatometric techniques to record the transformation. The transformation time is again found to depend inversely on the heating rate, and the isothermal transformation temperature is quoted as 926°C at 900°C per second, 928°C at 430°C per second, indicating that there is no rate-dependence of the transformation temperature.

The present investigation is concerned with the $\alpha \rightarrow \gamma$ transformation in Armco iron, and was instigated by the idea of a possible analogy with the transition from diffusion-controlled to diffusionless mechanisms on increasing the cooling rate, in iron of various carbon contents. The nature of the martensitic transformation in iron-carbon alloys has been the subject of much controversy. * In view of the clear indication from the preceding review that the prior structure - viz., ferrite, and the mode of distribution of carbide therein - is of primary importance in determining the nature of the transformation on rapid heating, the analogy with the reverse transformation will not be pursued in detail.

---

* See, for example, Radcliffe et al (1962), Singh and Parr (1962).

# 2: EXPERIMENTAL PROCEDURE

The problem of obtaining heating rates of several thousand degrees (Centigrade) per second, and at the same time measuring the temperature accurately throughout the heating range, led to the investigation of a number of experimental techniques, which can be divided into three groups, as follows:

2.1 Indirect (radiative) heating, with temperature measurement by thermocouple.

2.2 Internal (electrical) heating, with temperature measurement by photoconducting device.

2.3 Internal (electrical) heating, with temperature measurement by thermocouple.

It would be possible to obtain high heating rates, simply by using a gas flame and a small specimen, but the problems of rate-control and temperature-measurement in such an environment seem to rule out this approach.

## 2.1 Radiative Heating

Two lines of investigation were followed. In the first of these, a small "flake" of iron was suspended by thermocouple wires inside a tantalum foil cylinder, and heated by passing a large current through the cylinder. The arrangement is shown schematically in figure 2.1.

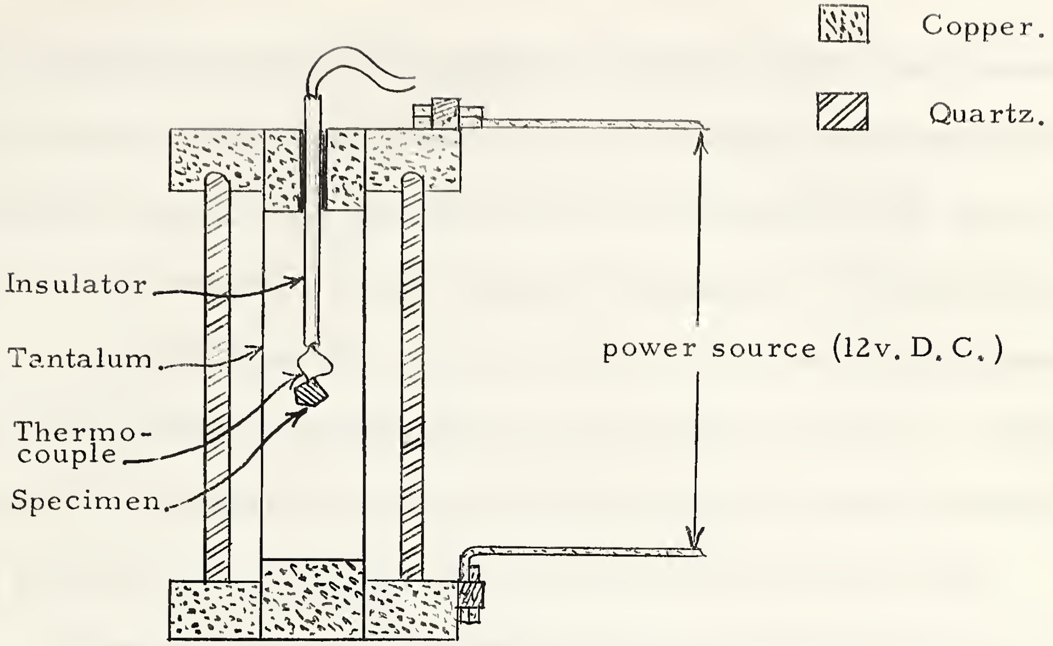

Figure 2.1 Trial radiative heating unit (tantalum foil furnace).

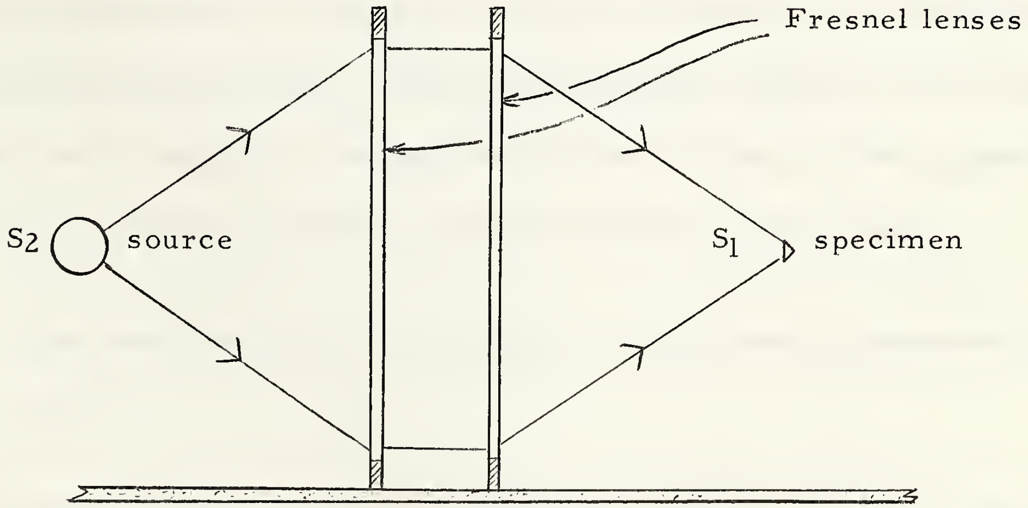

Figure 2.2 Trial radiative heating unit (Fresnel lens system).

The method was successful for heating rates up to 1000°C per second, but to produce higher rates it was found necessary to use specimens of so small a size that the thermal arrest corresponding to the $\alpha \longrightarrow \gamma$ phase transformation became difficult to distinguish. The method seems to be inapplicable for this reason, in spite of the possibility of improving the heating rates by suitable design of the furnace geometry. Furthermore, it was possible to exercise only the coarsest control over the heating rate, and the temperature versus time curve was non-linear.

A second approach to the radiant heating method was to place a small specimen at one focus S1 of the optical device illustrated in figure 2.2. Various methods of providing the heat source at the other focus S2 were investigated; for example, striking an electric arc or placing an infra-red heat lamp at S2. None proved intense enough to produce the heating rates required, presumably because in principle both a point source and a point target are needed for efficient heat transfer.

## 2.2 Electrical Heating. (Temperature measurement by photoelectric cell.)

Internal electric heating, by passing a large current through a specimen in wire form, appears to have a number of advantages over the methods described above. For example an almost linear heating curve should be obtained by applying a constant voltage to the specimen, and

accurate control of the heating rate should be possible by suitable regulation of the power supplied to the specimen. The use of a photoconducting device to measure the radiation emitted by the specimen (and hence its temperature) should confer the additional advantage that the temperature-measurement circuit is electrically independent of the heating circuit. This advantage - as the preliminary work, described below, on the use of thermocouples to measure the temperature, seemed to indicate - might very well be crucial.

However, the use of a photoconducting device, though elegant in principle, suffers from three major drawbacks. The first of these is the problem of calibration; if thermocouples are used to calibrate the temperature-response of the device, it seems that they will not provide an accurate reading of temperature (v.i.) if the specimen is heated electrically; therefore the conditions during the calibration will be different from those pertaining to the actual experiment. Second, it was found that with the photo-duo-diode used (Texas Instruments, type HB5) no appreciable response occurred below about 850°C, making it impossible to measure the heating rate below this temperature. Third, the curve of the e.m.f. response versus time obtained was extremely nonlinear, so that the estimation of the heating rate was difficult for any given temperature.

## 2.3 Electrical Heating. (Temperature measurement by thermocouple.)

The three drawbacks outlined above would be removed if the temperature measurement could be made by using a thermocouple instead of the photoelectric device; at the same time the advantages of the electrical heating method would be retained.

Preliminary attempts employed a simple series circuit, containing a twelve-volt battery as the power source, a variable resistor to control the heating rate, a fast-acting magnetic switch, and an iron specimen in wire form. The thermocouple was spot-welded to the specimen, and connected to a recorder, by means of which the variation of the e.m.f. across the thermocouple leads could be measured. The technique proved to be unsatisfactory, because of stray electrical pick-up (in addition to the thermal e.m.f.) which appeared across the thermocouple leads on closing the switch. This pick-up increased non-linearly according to the power supplied to the specimen. Thus accurate measurement of the temperature was impossible. Several modifications of the basic arrangement were made, without success, namely:

(1) Variation of the length or diameter of the specimen.

(2) Variation of the diameter of the thermocouple wires.

(3) Variation of the position of the weld on the specimen.

(4) Welding the two thermocouple wires on opposite sides of the specimen, as far as possible in the same lateral plane.

(5) Using various pairs of metals to make up the thermocouple.

It was found that the stray e.m.f. increased as the spacing, between the points of contact of the two thermocouples with the specimen, was increased along its length. Thus the pick-up was due to the finite separation of these points of contact, which did not, as a result, lie in an equipotential plane of the specimen.

The solution to the problem consisted in the use of a simple balancing circuit devised by Boedtker and Duwez (1962) and shown schematically in figure 2.3. Three thermocouple wires were welded to the specimen at a spacing of about .010 inches; if the centre wire was, say, chromel, and the outer ones alumel, the arrangement would constitute a double thermocouple. (The macrostructure of the welds, using 0.003 inch diameter thermocouple wires and a specimen of about .050 inches diameter, is shown in figure 2.4.) The two outer wires were then connected across the fixed contacts of a 10-ohm potentiometer (Heliopot, model A) and the moveable contact adjusted until, on passing a low current through the specimen, no discontinuity occurred in the e.m.f. recorded between the chromel wire and the moveable contact - the latter being at a potential representing the average for the two alumel wires. In this way any non-thermal contribution to the recorded e.m.f. was eliminated.

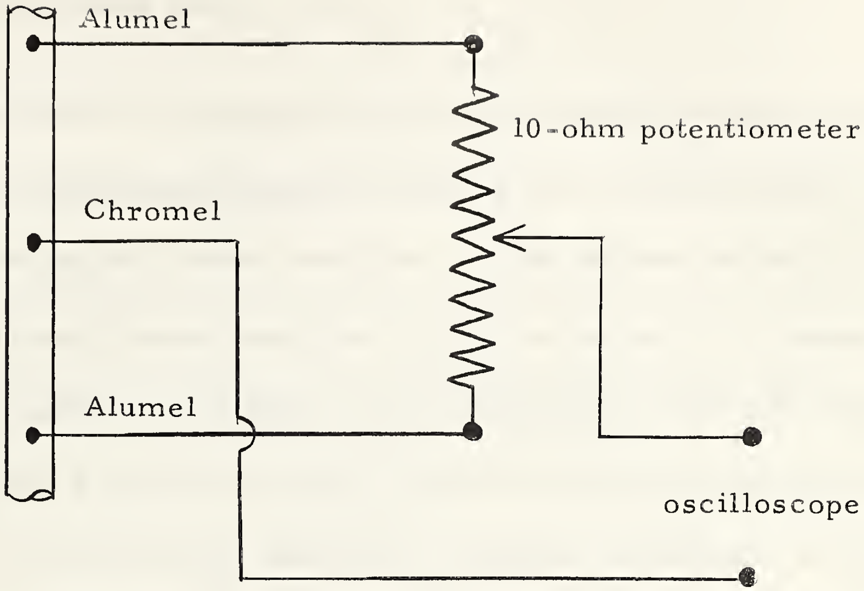

Figure 2.3 Balancing circuit (after Boedtker and Duwez).

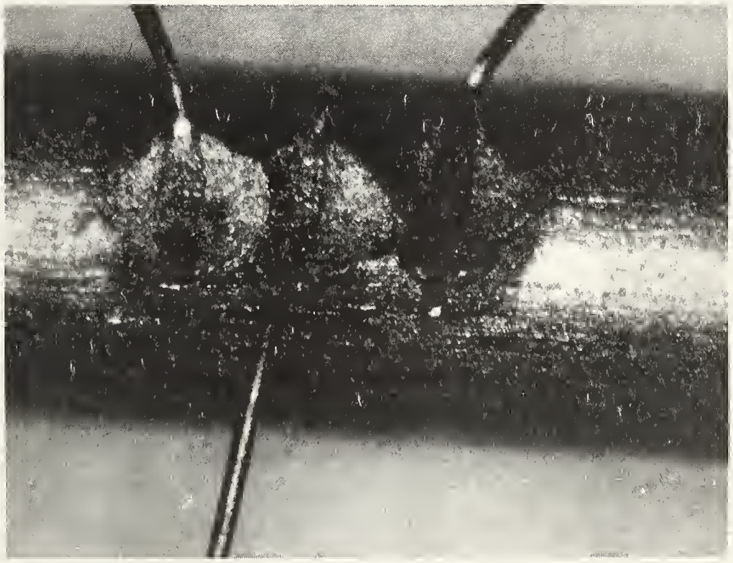

Figure 2.4 Macrostructure of a thermocouple weld. (x 30)

## 2.4 The Heating Unit

An order-of-magnitude calculation showed that 1000 amps delivered at twelve volts should produce a heating rate of about 10,000°C per second for specimens of a convenient size. (A description of the factors influencing the choice of specimen size is given in section 2.6, below.) A high-current supply such as this is most conveniently obtained from a D.C. source, and a primary heating circuit was therefore set up using four twelve-volt wet storage batteries, connected in parallel, as the power supply. A slide-wire resistor was used as a rate controller, and a heavy solenoid switch ensured that the circuit could be closed rapidly. This arrangement provided a heating range from 500°C to about 6000°C per second for specimens two inches in length; shorter specimens were used to obtain faster rates (up to about 20,000°C per second); and for rates below 500°C per second a secondary circuit, consisting of a single battery and a carbon-block rheostat, was used. The secondary circuit also provided a means of holding a specimen at 800°C for one minute before the application of the final heating pulse, and this technique was used in a subsidiary series of experiments, oxidation of the specimen being prevented by means of a protective helium atmosphere.

The balancing circuit for the thermocouples consisted of a twelve-volt battery, a fixed one-ohm resistor, and a switch enabling the current direction along the specimen to be reversed. The heating and auxiliary

circuits are shown in figure 2.5, and a schematic drawing of the unit is given in figure 2.6.

## 2.5 Recording the Heating Curve

A photographic record of the temperature versus time curve for each specimen was obtained, by connecting the "balanced" e.m.f. output from the thermocouples across an oscilloscope (Tektronix type 502A) fitted with a camera (Tektronix type C12, with Polaroid land camera back). Slow rates were recorded on a Bausch and Lomb strip chart recorder. Three typical oscillograph curves are shown in figure 2.7; inspection shows that the thermal arrest, corresponding to the absorption of latent heat during the $\alpha \rightarrow \gamma$ transformation, is clearly visible. There was little difficulty in estimating the position of this arrest on the curve even at rates well in excess of 10,000°C per second; a full description of the measurement of the various parameters from these curves is given in part 5.2 of the appendix.

It was found necessary to "float" the whole heating and recording apparatus with respect to ground, since otherwise the oscilloscope would record the "true" voltage at the hot thermocouple junctions, and not the change in voltage caused by heating alone.

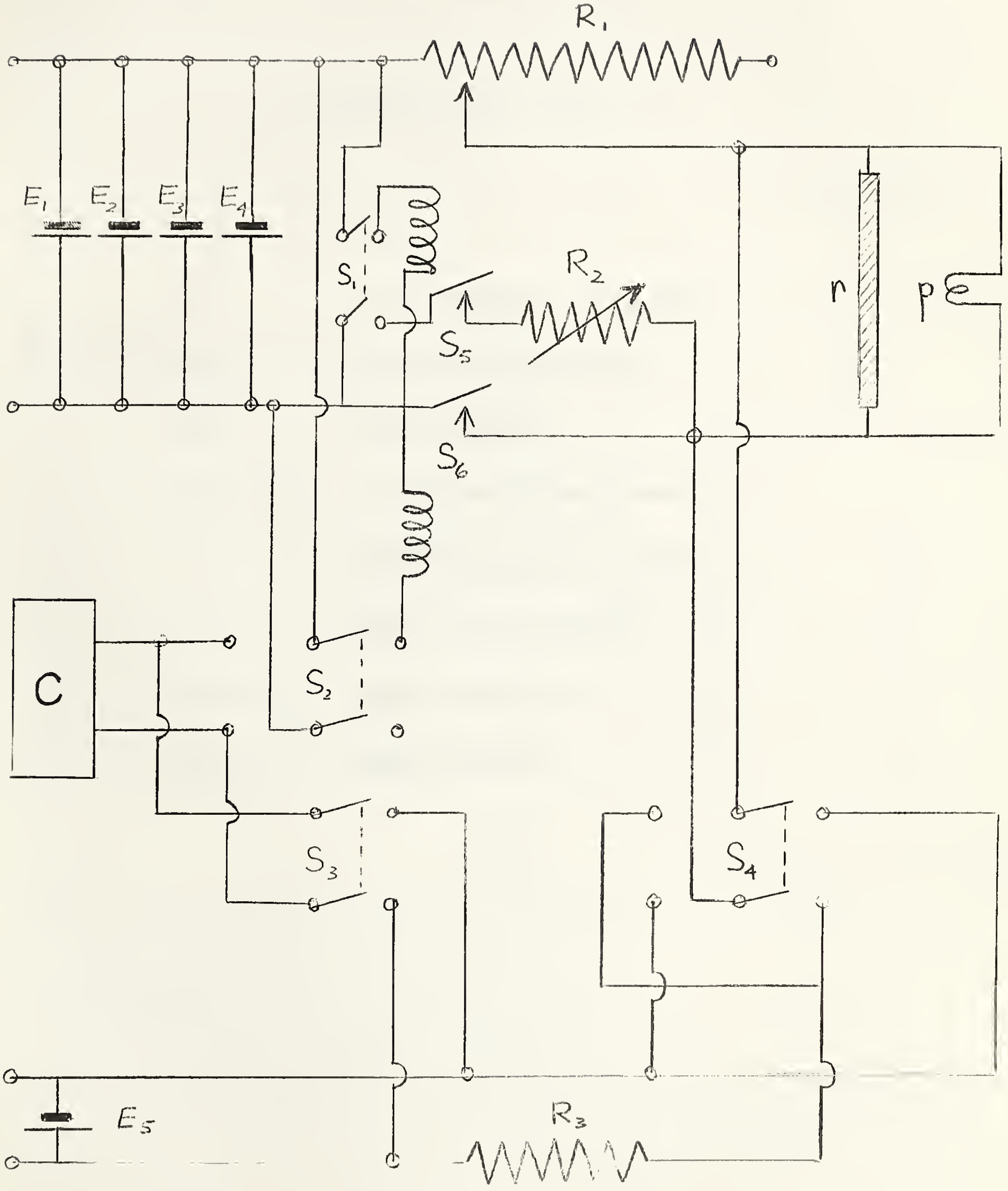

Figure 2.5 The heating and auxiliary circuits (see also next page).

Symbols used in figure 2.5

| | |
|---|---|
| $r$ | load |
| $R_1$ | rate-controlling resistor |
| $R_2$ | carbon-block rheostat |
| $R_3$ | 1-ohm resistor |
| $E_1$ -- $E_5$ | 12-volt wet storage batteries |
| C | trickle charger for batteries |
| p | power warning light |
| $S_1$ -- $S_4$ | toggle switches |
| $S_5$, $S_6$ | relay switches |

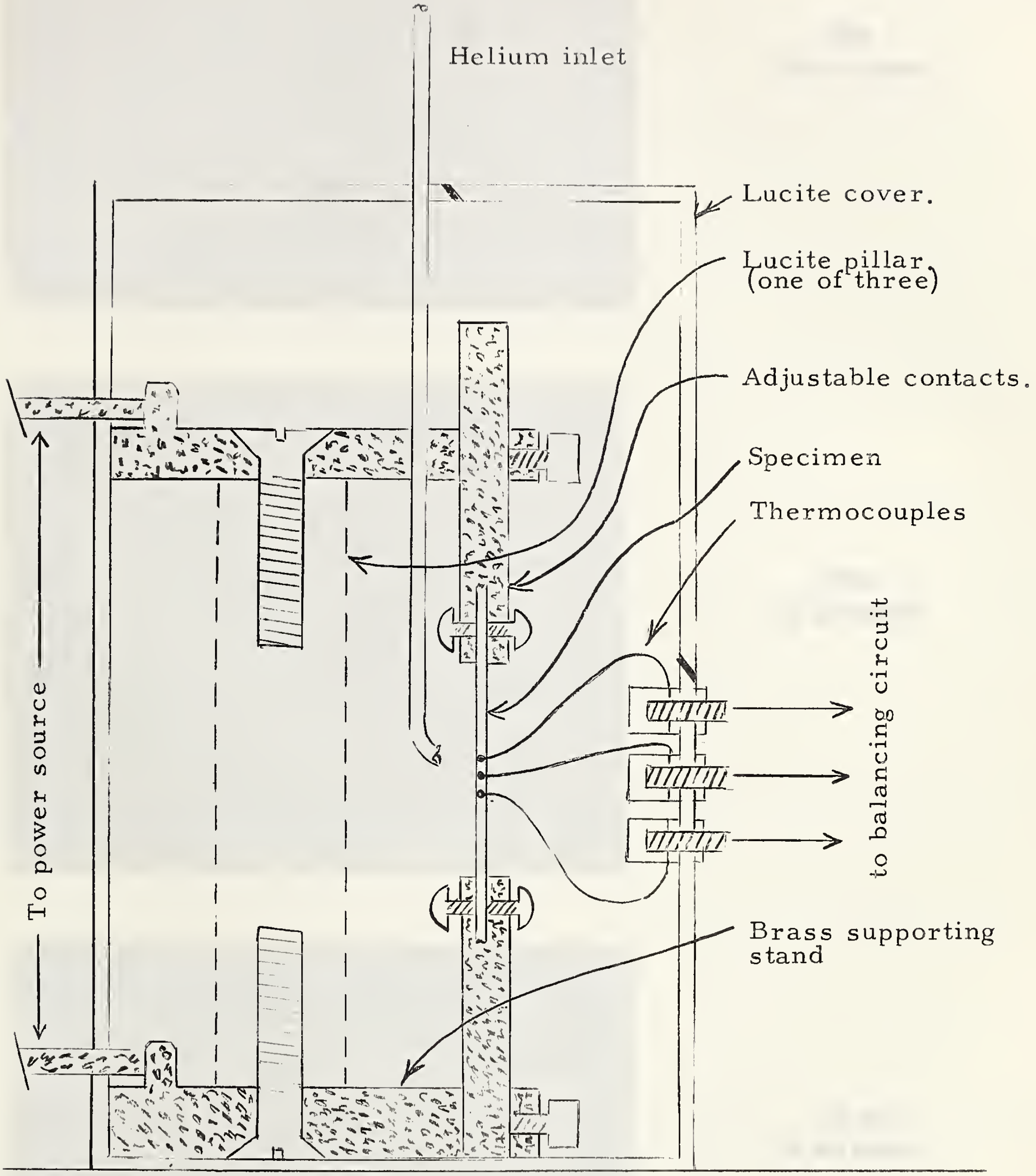

Figure 2.6 Schematic drawing of the heating unit.

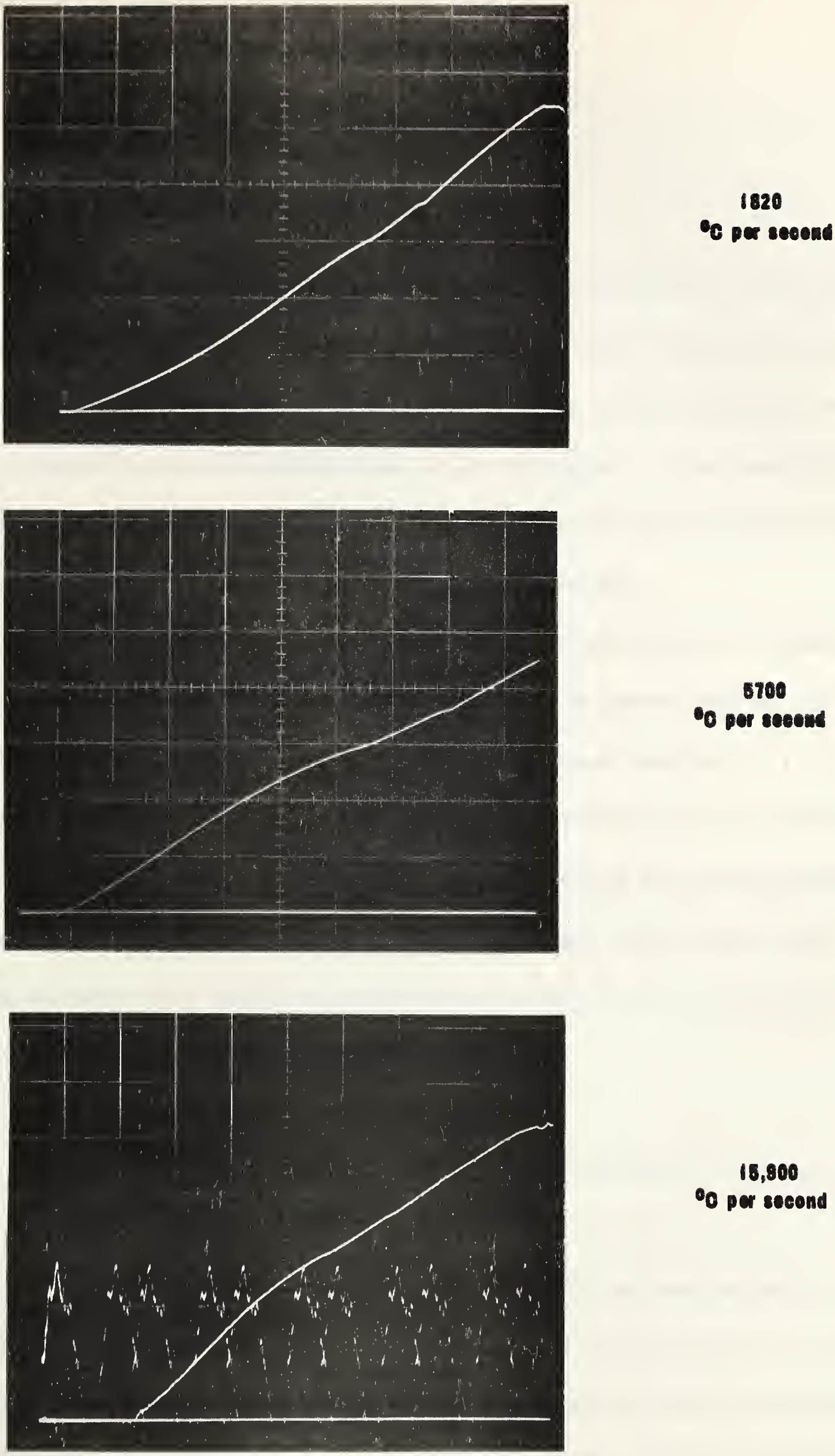

1820
°C per second

5700
°C per second

15,900
°C per second

Figure 2.7 Three typical heating curves.

## 2.6 Preparation of Specimens

Consideration of reasonable power requirements, clarity of the thermal arrest on the heating curve, and general robustness for handling and welding, led to a choice of specimen size of approximately two inches in length by one-twentieth of an inch in diameter. The possibility that a skin-effect might arise in wires of this diameter has been ignored because of the low-frequency nature of the applied voltage.

The material used was Armco iron, supplied by A. D. MacKay and Company of New York, as cold-drawn wire of approximately .050 inches diameter. (A spectrographic analysis is given in table 2.1.) The wire was cleaned in alcohol, hand-straightened, and cut into two and a half inch lengths. Experiments were also conducted on annealed samples of the same wire; after cleaning, straightening, and cutting to size, these specimens were annealed in batches of twenty-five for six hours at the following temperatures:

A $600^{\circ}$C )
)
B $800^{\circ}$C ) followed by "furnace-cooling"
)
C $1000^{\circ}$C )

Representative microphotographs of the specimens are reproduced in figures 2.8 to 2.11. Annealing was carried out in a Vitreosil tube sealed at one end, which was placed in an electrical resistance furnace whose temperature could be controlled to plus or minus $5^{\circ}$C, and

## TABLE 2.1

| Element | Weight per cent |
|---|---|
| Carbon | 0.030 * |
| Chromium | 0.01 |
| Copper | 0.07 |
| Manganese | 0.03 |
| Nickel | 0.05 |
| Nitrogen | 0.0045 |
| Oxygen | 0.108 |
| Phosphorus | 0.010 |
| Silicon | <0.005 |
| Sulphur | 0.014 |

MATERIAL: Armco iron "as received"

* 0.020 weight per cent after annealing in vacuo for 6 hours at 1000°C.

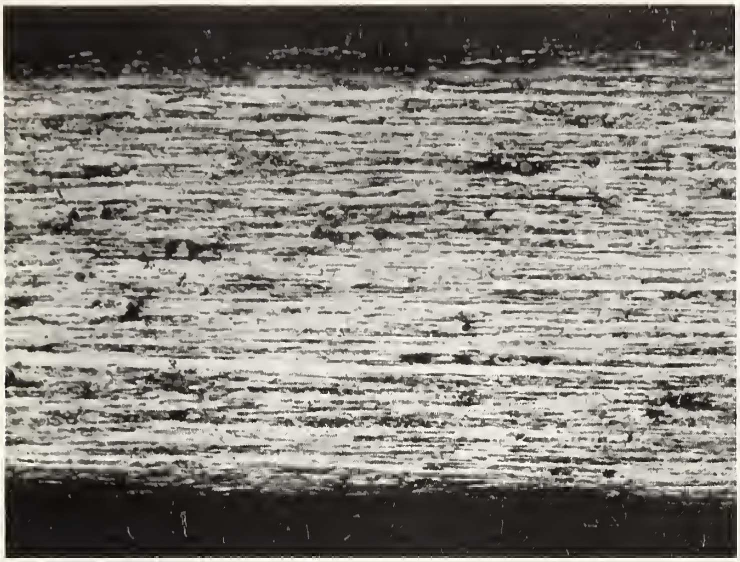

Figure 2.8 Microstructure of a cold-worked specimen (x 100)

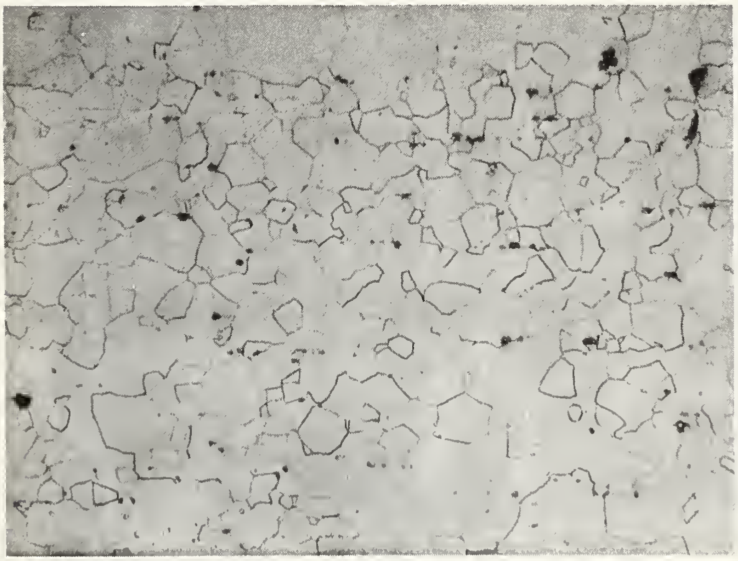

Figure 2.9 Microstructure of a specimen annealed at 600°C. (x100)

[illegible]

[illegible]

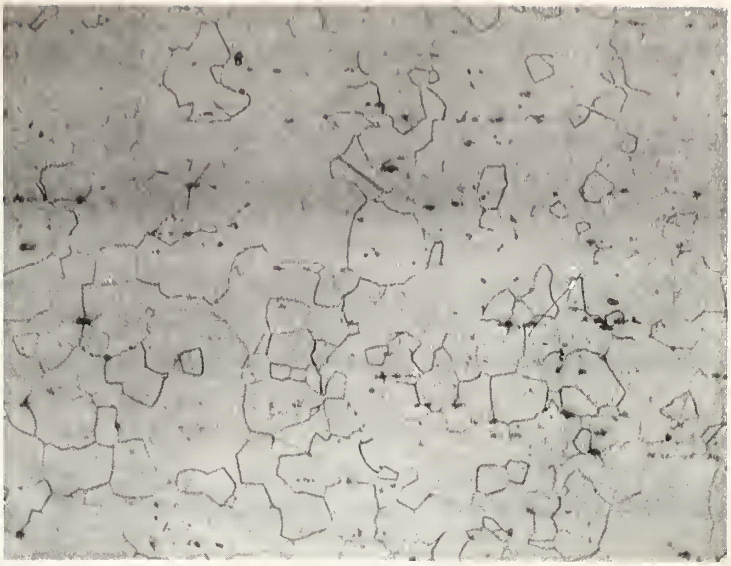

Figure 2.10 Microstructure of a specimen annealed at 800°C. (x 100)

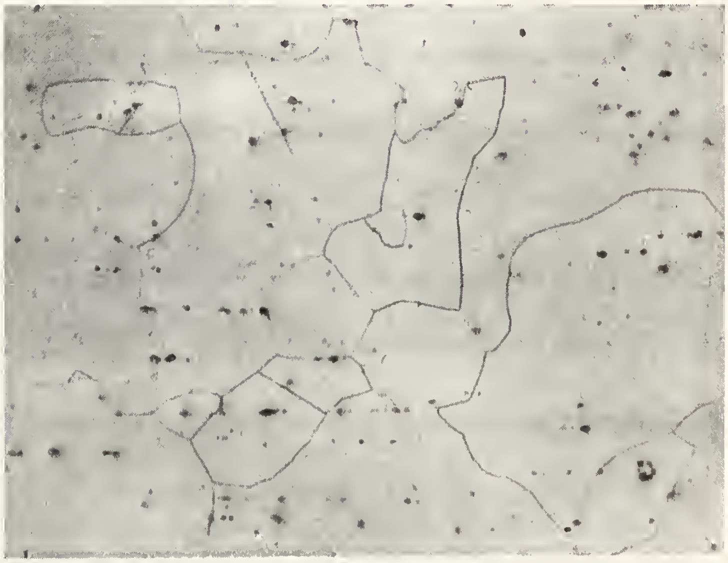

Figure 2.11 Microstructure of a specimen annealed at 1000°C. (x 100)

[illegible]

[illegible]

evacuated to better than $10^{-6}$ millimetres mercury by means of an eight-inch oil diffusion pump backed by a mechanical pump. Contamination from the walls of the tube was avoided by the use of a stand of Armco iron to hold the specimens. (The effect of specimen contamination was noticed after annealing in imperfectly-sealed tubes under the passage of argon gas.) Some experiments were also performed on annealed steel of .049 inches diameter whose composition is given in table 2.2.

2.7 A number of steps were taken to ensure the accuracy of the temperature-measurement techniques described in section 2.3 above. These were as follows:

(1) The effect of possible contamination during the heating period itself was investigated, by performing a comparable series of experiments in air and under a protective helium atmosphere.

(2) The effect of any systematic spurious electrical pick-up, caused by thermal gradients along the specimen, or any unspecified "nonthermal" pick-up, was investigated by reversing the thermocouple arrangement, i.e. using chromel-alumel-chromel instead of alumel-chromel-alumel leads.

(3) The possibility of stray pick-up at high temperatures was further investigated by using "dummy" alumel-alumel-alumel and chromel-chromel-chromel leads.

## TABLE 2.2

| Element | Weight per cent |
|---|---|
| Carbon | 0.94 |
| Manganese | 0.53 |
| Phosphorus | 0.014 |
| Silicon | 0.20 |
| Sulphur | 0.018 |

MATERIAL: Steel "as received."

(4) Platinum versus platinum-ten per cent rhodium thermocouples were used for some heating runs. The extensive use of this method was discouraged by the tendency of the thermocouple wires to become detached from the specimen at relatively low temperatures.

(5) Etched, polished, and untreated samples of the cold-worked specimens were investigated to determine the effect of surface condition.

# 3. RESULTS

## 3.1 The Transformation Temperature.

The results of the rate-of-heating experiments are presented graphically in figures 3.1 to 3.6, in the form of plots of Curie temperature and transformation temperature versus heating rate,* for Armco iron. The corresponding data are given in tables 3.1 to 3.6. The transformation temperature versus heating rate* curve for the annealed steel specimens is reproduced in figure 3.7 (rate values on logarithmic scale), using the data from table 3.7.

## 3.2 The Transformation Time.

Figures 3.8 and 3.9 (tables 3.1, 3.5) show the dependence of the transformation time* on the heating rate, for cold-worked Armco iron heated from room temperature (figure 3.8) and from 800°C (figure 3.9). The heat-treatment history of the samples corresponding to each of the figures 3.1 to 3.9 is summarized in table 3.0.

## 3.3 The Latent Heat of Transformation.

The latent heat of transformation, L, was calculated for Armco

---

* The method of determining the transformation temperature and time, and heating rate, from a given experimental curve, is described in section 5.2 of the appendix.

iron fromthe data of tables 3.1 and 3.5, by determining the value of the parameter $s\tau$ for each pair of readings; the calculation is explained in section 5.4 of the appendix, and produced the following results:

(a) From table 3.1 (figure 3.8),

$$L = 3.7, \text{ s.d.}^* \ 0.7, \text{ cal. per gm.}$$

(b) From table 3.5 (figure 3.9),

$$L = 3.2, \text{ s.d.}^* \ 0.6, \text{ cal. per gm.}$$

### 3.4 Subsidiary Results.

A small number of results, for heating speeds in the range 300°C per second to about 1200°C per second, were obtained by the radiative heating method described in section 2.1. Some typical values are given in table 3.8, and the composition of the material used is included.

In many of the experiments involving fairly slow heating of the Armco iron specimens, it was possible to switch off the power supply to the specimen before the latter melted, and record a cooling curve including the temperature of the $\gamma \rightarrow \alpha$ transformation. Cooling rates ranged

---

* Standard deviation from the mean.

from about 100°C per second to 300°C per second, and the $\gamma \longrightarrow \alpha$ transformation temperature always fell between the limits 885°C and 865°C.

Note on Figures 3. 1 to 3. 6:

The symbols ○, ● denote results obtained using alumel and chromel, respectively, as the central thermocouple lead.

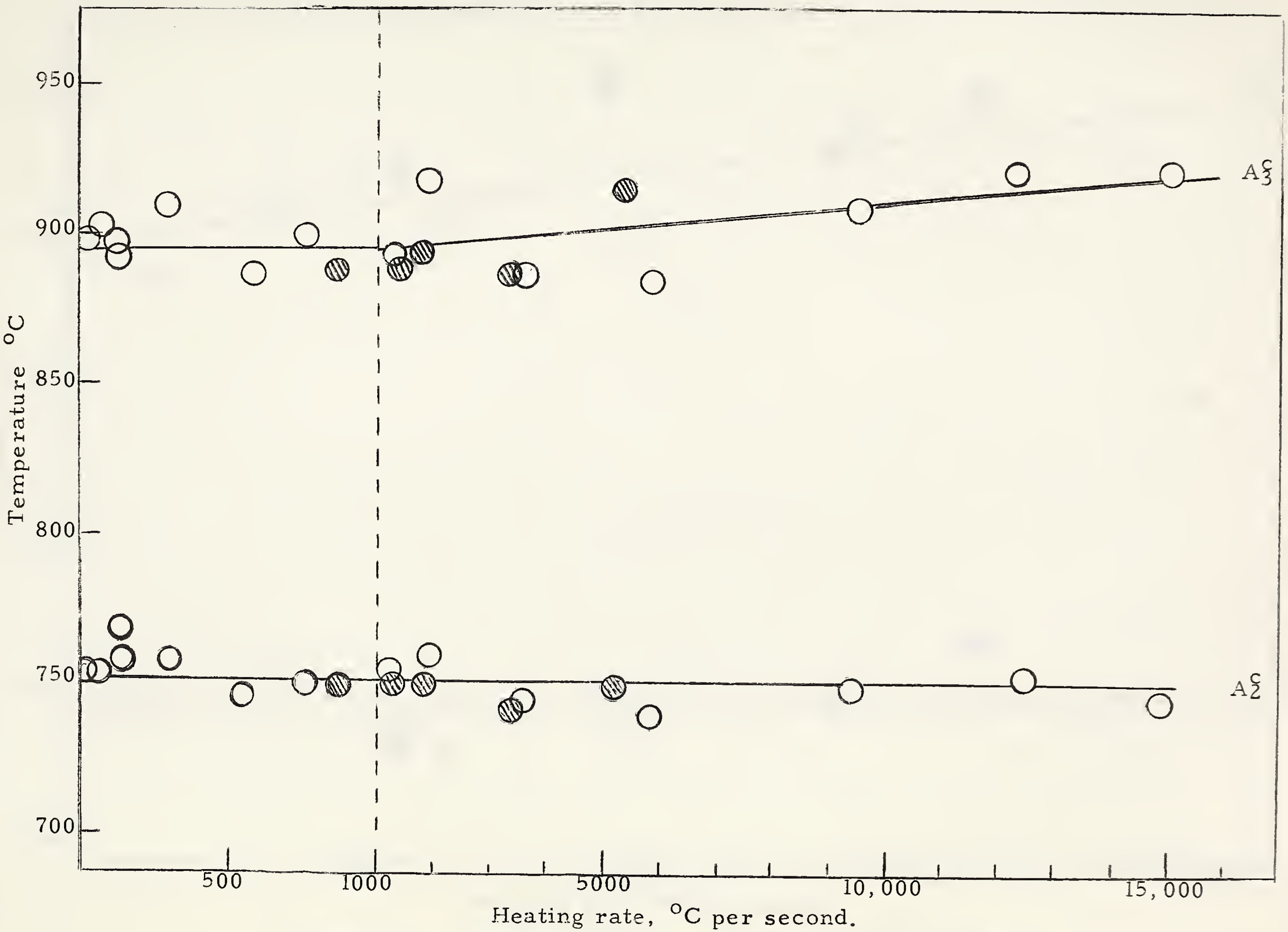

Figure 3.1 Rate data, for cold-worked Armco iron.

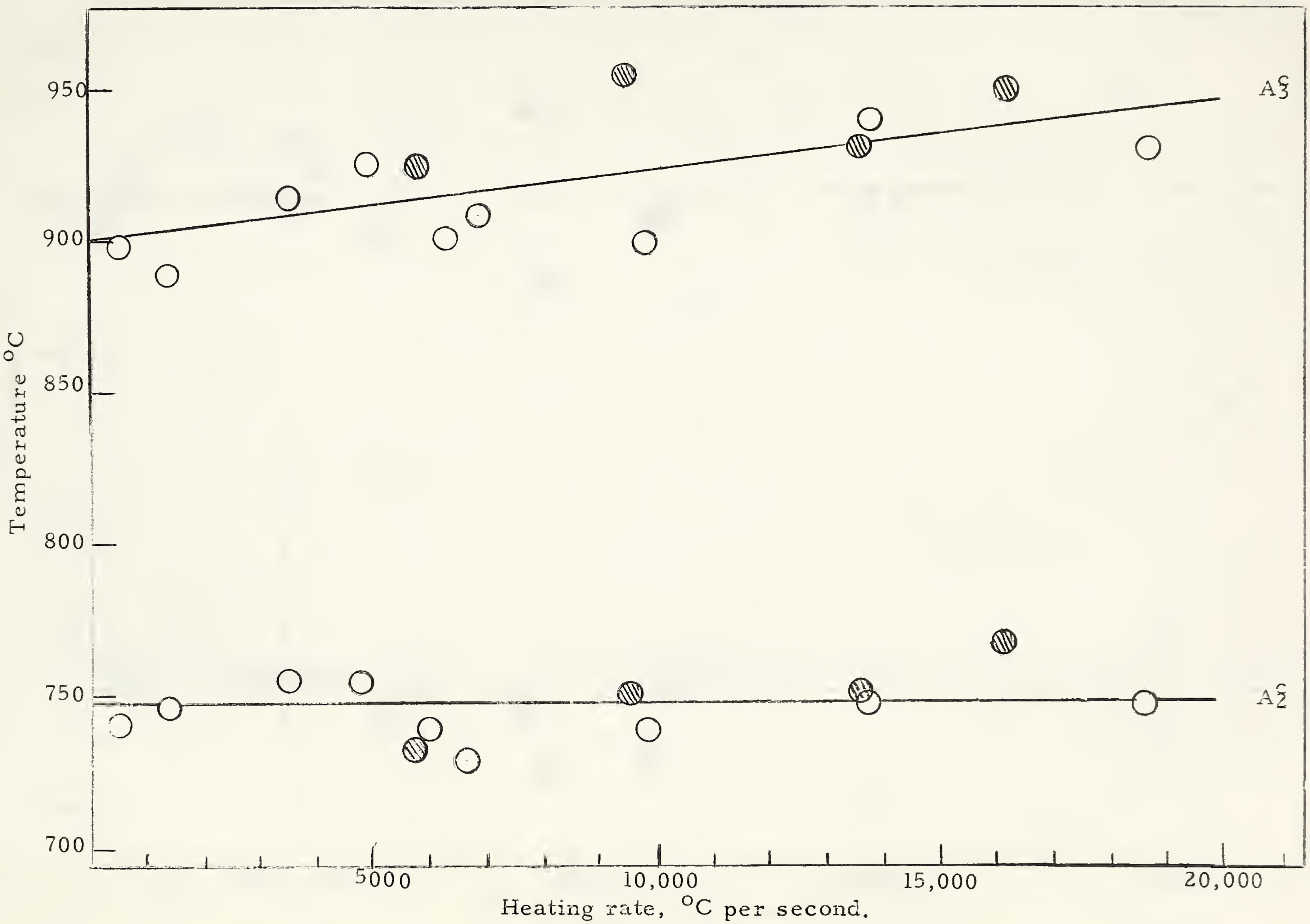

Figure 3.2 Rate data, for Armco iron annealed at 600°C.

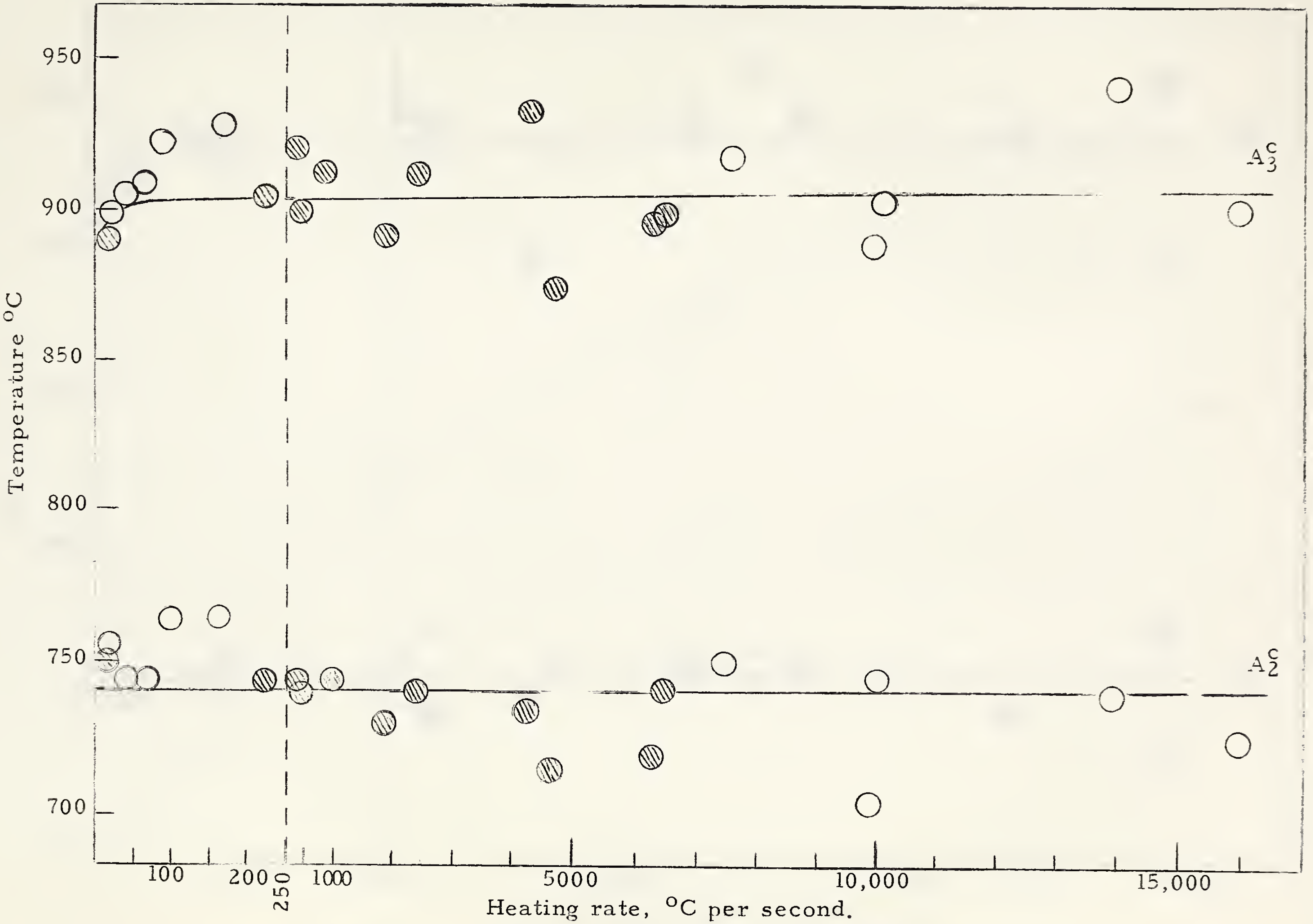

Figure 3.3 Rate data, for Armco iron annealed at 800°C.

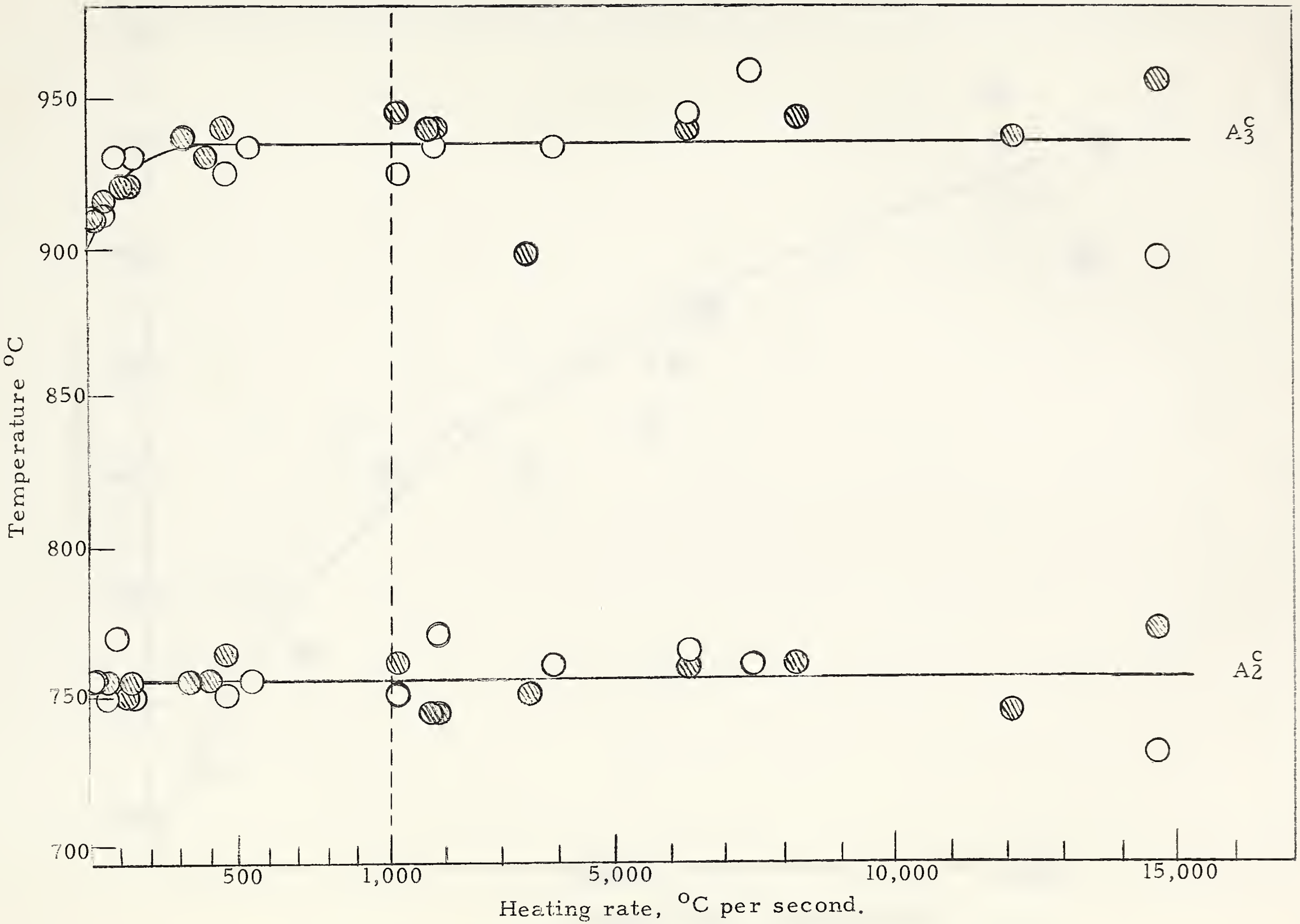

Figure 3.4 Rate data, for Armco iron annealed at 1000°C.

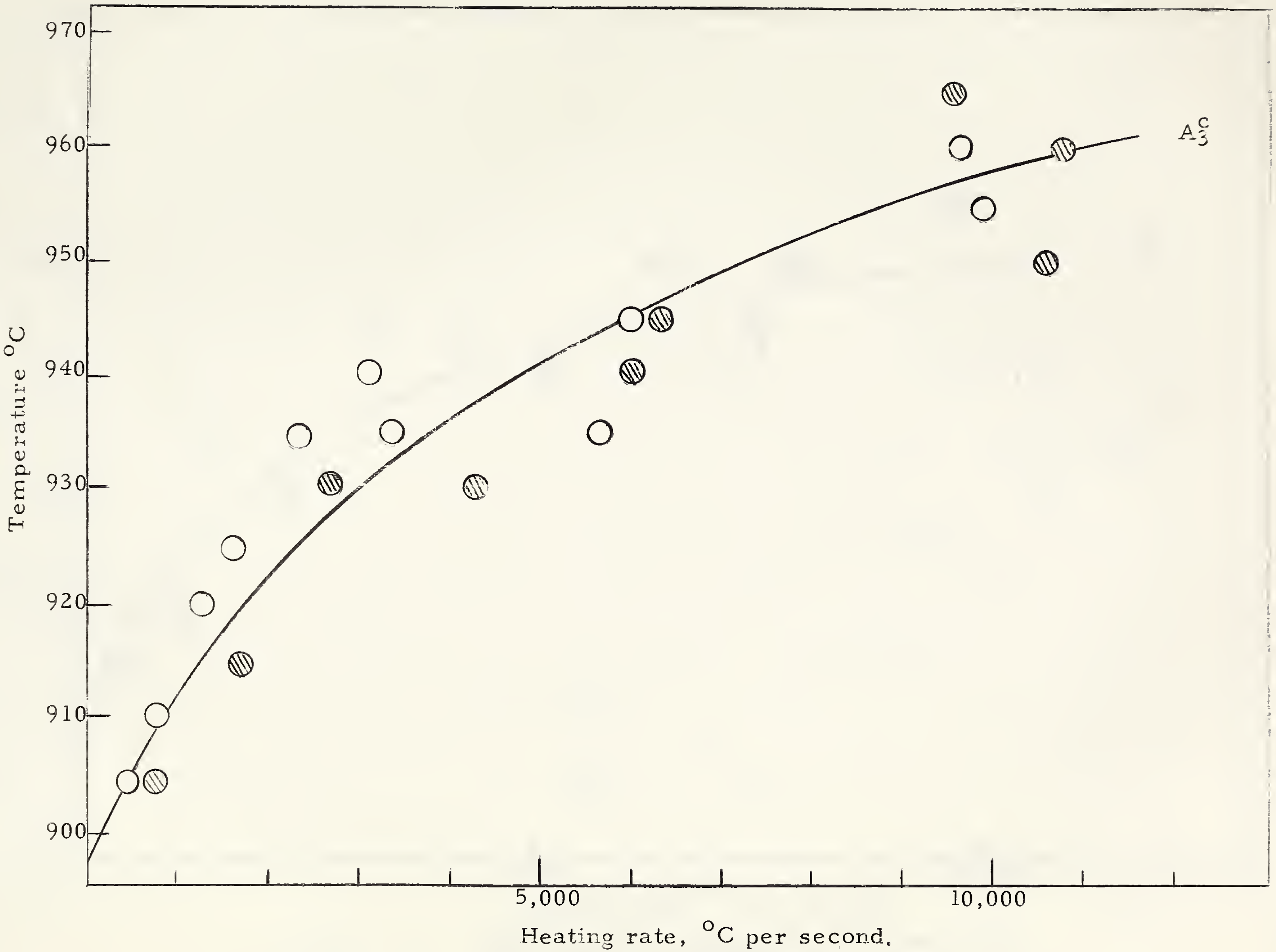

Figure 3.5 Rate data for cold-worked Armco iron held 1 minute at 800°C.

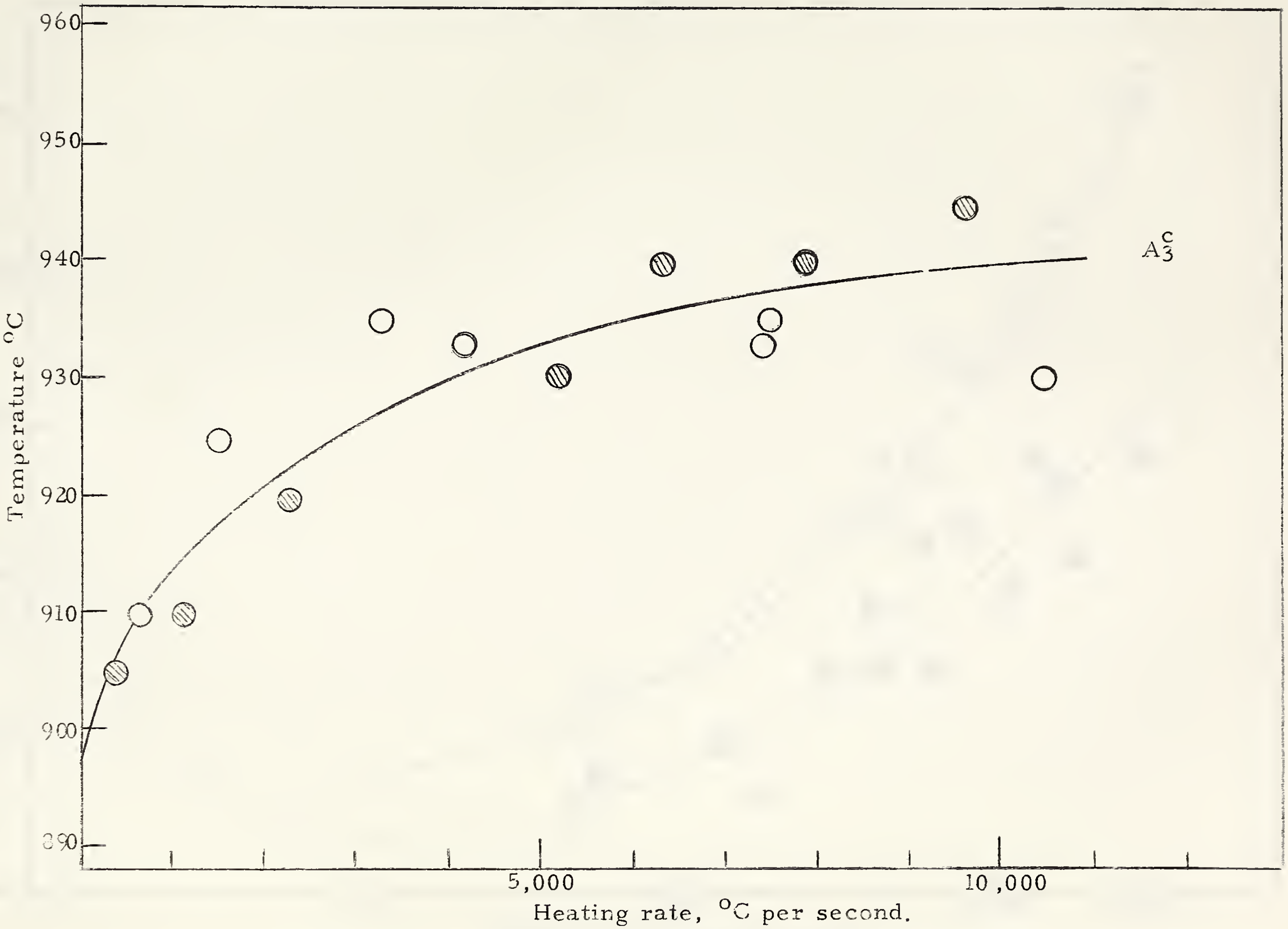

Figure 3.6 Rate data for annealed ($800^0C$) Armco iron held 1 minute at 800°C.

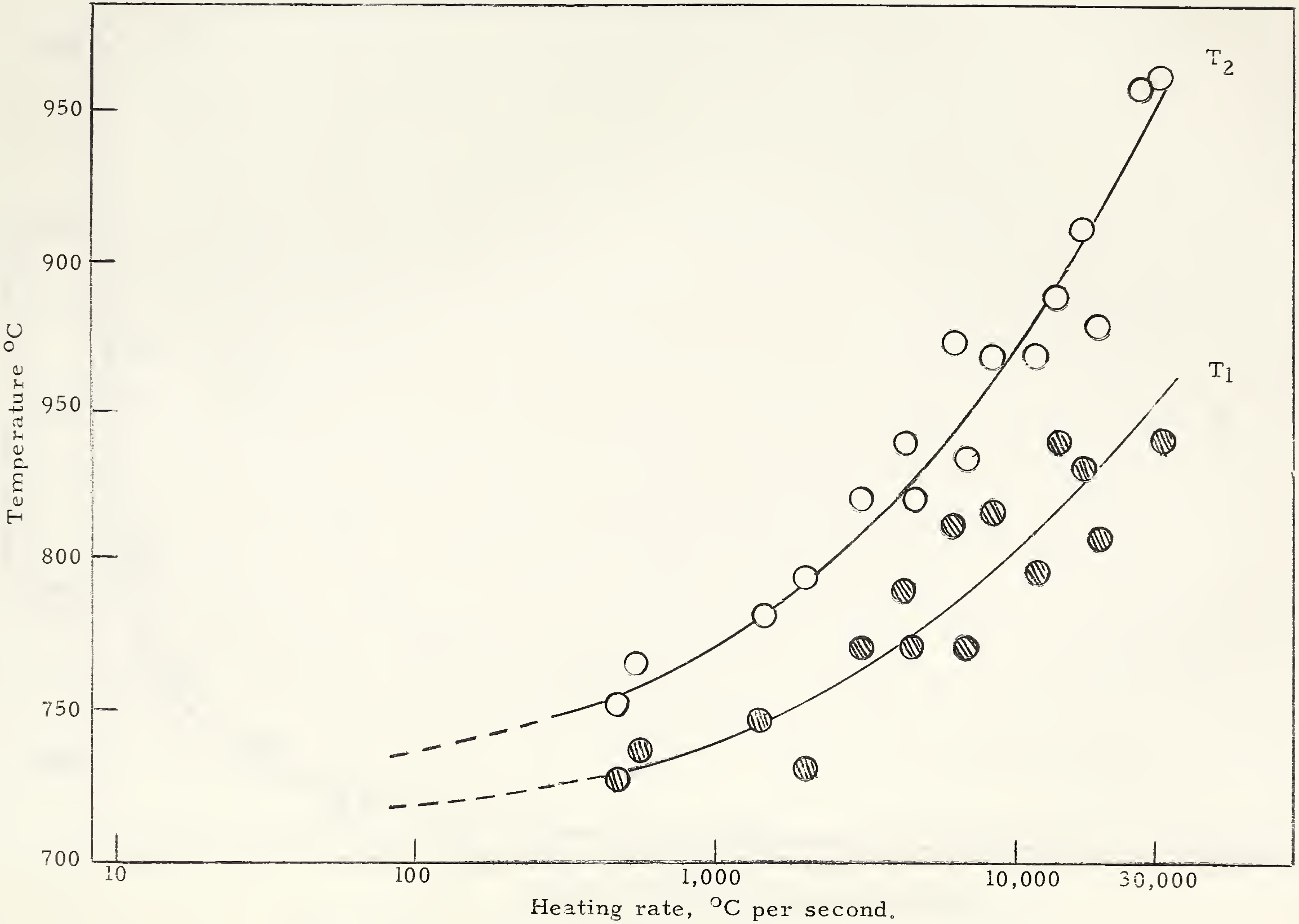

Figure 3.7 Rate data for annealed steel (logarithmic rate scale).

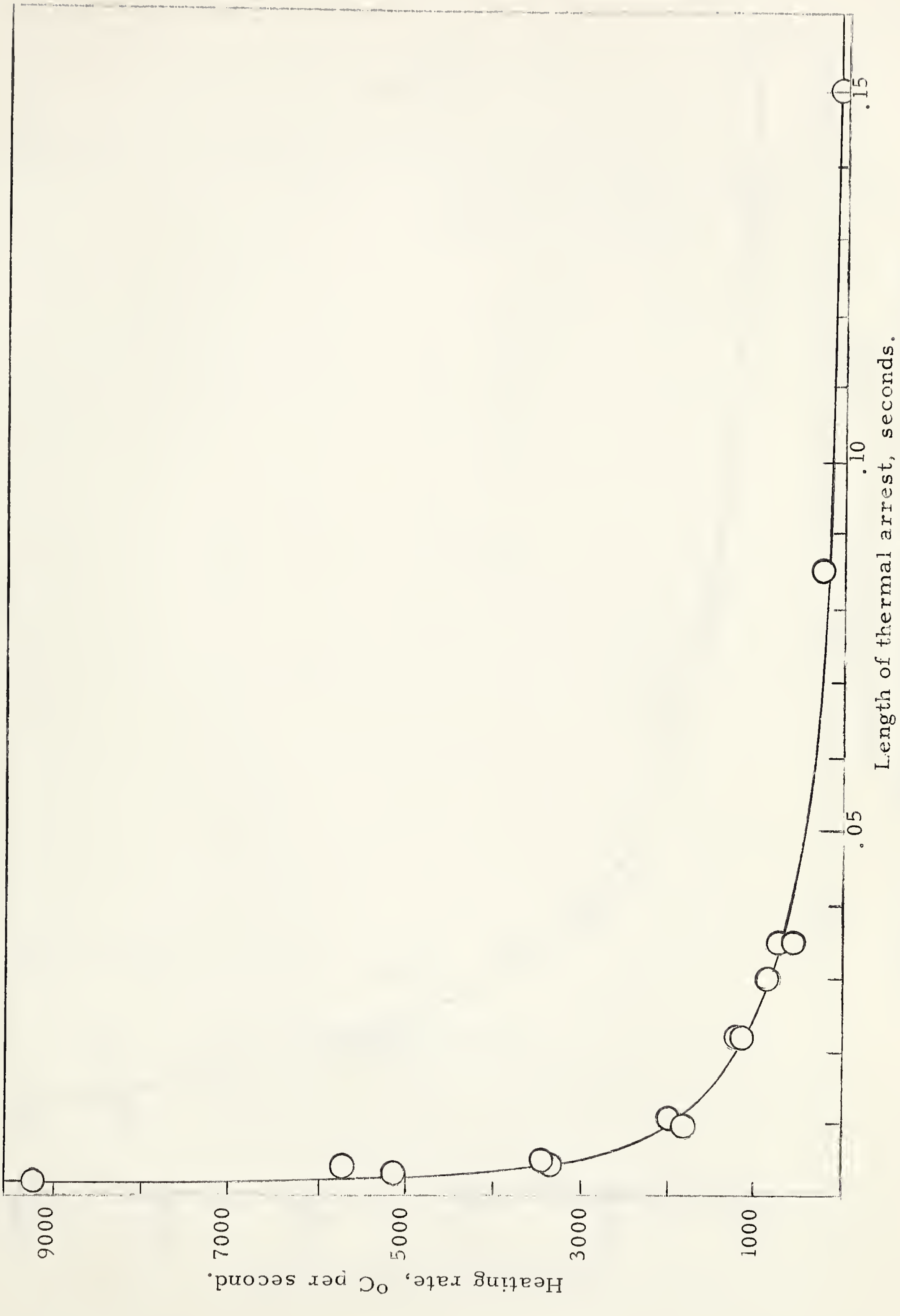

Figure 3.8 Data for cold-worked Armco iron heated from room temperature.

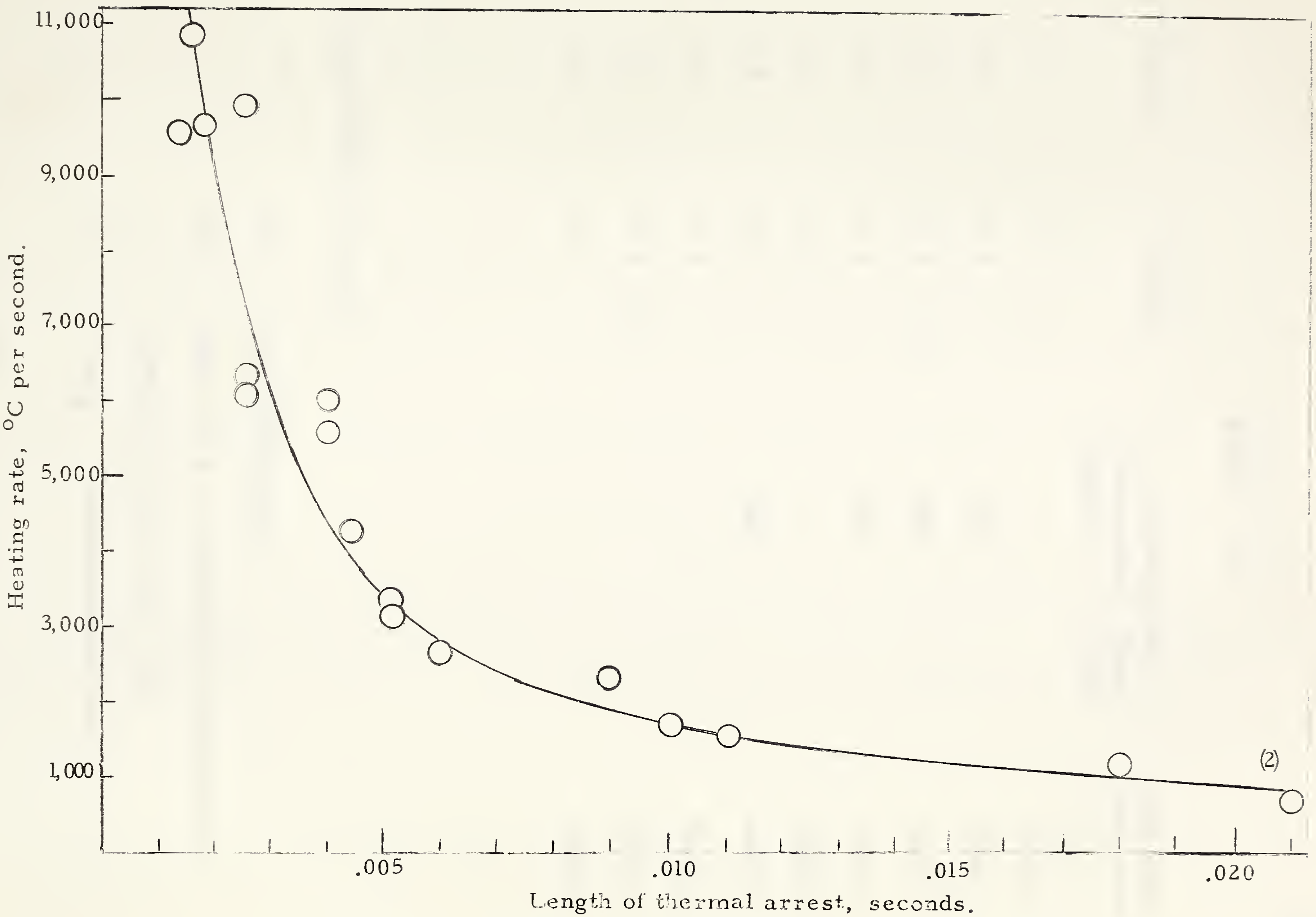

Figure 3.9 Data for cold-worked Armco iron heated from 800°C after 1 minute holding.

## TABLE 3.0

| TABLE | FIGURE | | ANNEALING | | HOLDING |
|---|---|---|---|---|---|
| | | | Temperature Degrees C. | Time, Hours | Temperature |
| 3.1 | 3.1 | 2.8 | - | - | Room |
| 3.2 | 3.2 | 2.9 | 600 | 6 | Room |
| 3.3 | 3.3 | 2.10 | 800 | 6 | Room |
| 3.4 | 3.4 | 2.11 | 1000 | 6 | Room |
| 3.5 | 3.5 | - | - | - | 800°C |
| 3.6 | 3.6 | - | 800 | 6 | 800°C |
| 3.7 | 3.7 | - | - | - | Room |
| 3.1 | 3.8 | 2.8 | - | - | Room |
| 3.5 | 3.9 | - | - | - | 800°C |

Key to tables 3.1 to 3.6:

| | |
|---|---|
| $A_2^c$ | Curie temperature. |
| $A_3^c$ | Mean $\alpha \rightarrow \gamma$ transformation temperature. |
| s | Heating rate from $A_2^c$ to $A_3^c$. |
| $\tau$ | $\alpha \rightarrow \gamma$ transformation time. |

## TABLE 3.1

| Number | $A_2^c$ degrees C | $A_3^c$ degrees C | s degrees C per second | $\tau$ seconds |
|---|---|---|---|---|
| 1 | 755 | 898 | 19 | - |
| 2 | 755 | 903 | 64 | .30 |
| 3 | 770 | 898 | 133 | .15 |
| 4 | 760 | 893 | 134 | - |
| 5 | 760 | 910 | 316 | .085 |
| 6 | 745 | 888 | 560 | .035 |
| 7 | 750 | 900 | 780 | .035 |
| 8 | 750 | 890 | 850 | .030 |
| 9 | 755 | 895 | 1150 | .022 |
| 10 | 750 | 890 | 1180 | .022 |
| 11 | 750 | 895 | 1820 | .010 |
| 12 | 765 | 920 | 1970 | .011 |
| 13 | 740 | 890 | 3380 | .0045 |
| 14 | 745 | 890 | 3500 | .0050 |
| 15 | 745 | 918 | 5150 | .0030 |
| 16 | 740 | 888 | 5700 | .0040 |
| 17 | 750 | 913 | 9300 | .0020 |
| 18 | 755 | 923 | 12600 | .0016 |
| 19 | 745 | 923 | 14900 | .0020 |

MATERIAL: Armco iron, as received.

## TABLE 3.2

| Number | $A_2^c$ degrees C | $A_3^c$ degrees C | s degrees C per second |
|---|---|---|---|
| 1 | 740 | 898 | 500 |
| 2 | 745 | 885 | 1400 |
| 3 | 755 | 915 | 3570 |
| 4 | 755 | 925 | 4800 |
| 5 | 735 | 925 | 5670 |
| 6 | 740 | 900 | 5850 |
| 7 | 730 | 908 | 6550 |
| 8 | 750 | 955 | 9500 |
| 9 | 740 | 898 | 9700 |
| 10 | 750 | 930 | 13600 |
| 11 | 745 | 940 | 13700 |
| 12 | 765 | 950 | 16100 |
| 13 | 745 | 930 | 18600 |

MATERIAL: Annealed Armco Iron.

TABLE 3.3

| Number | $A_2^c$ degrees C | $A_3^c$ degrees C | s degrees C per second |
|---|---|---|---|
| 1 | 755 | 898 | 13 |
| 2 | 750 | 890 | 13 |
| 3 | 745 | 905 | 36.5 |
| 4 | 745 | 910 | 67 |
| 5 | 765 | 923 | 96 |
| 6 | 765 | 928 | 170 |
| 7 | 745 | 905 | 220 |
| 8 | 745 | 920 | 380 |
| 9 | 740 | 900 | 430 |
| 10 | 745 | 913 | 970 |
| 11 | 730 | 893 | 1750 |
| 12 | 740 | 913 | 2250 |
| 13 | 735 | 933 | 4150 |
| 14 | 715 | 875 | 4600 |
| 15 | 720 | 898 | 6200 |
| 16 | 740 | 900 | 6450 |
| 17 | 750 | 918 | 7300 |
| 18 | 705 | 890 | 9800 |
| 19 | 745 | 905 | 9900 |
| 20 | 740 | 940 | 13800 |
| 21 | 735 | 903 | 15900 |

MATERIAL: Annealed Armco iron.

## TABLE 3.4

| Number | $A_2^c$ degrees C | $A_3^c$ degrees C | s degrees C per second |
|---|---|---|---|
| 1 | 755 | 910 | 17 |
| 2 | 755 | 909 | 22 |
| 3 | 755 | 919 | 45 |
| 4 | 750 | 910 | 51 |
| 5 | 770 | 930 | 90 |
| 6 | 750 | 921 | 105 |
| 7 | 755 | 920 | 120 |
| 8 | 750 | 930 | 130 |
| 9 | 755 | 937 | 315 |
| 10 | 755 | 930 | 390 |
| 11 | 765 | 940 | 465 |
| 12 | 750 | 925 | 465 |
| 13 | 755 | 933 | 535 |
| 14 | 760 | 945 | 1050 |
| 15 | 750 | 923 | 1050 |
| 16 | 745 | 940 | 1750 |
| 17 | 770 | 935 | 1800 |
| 18 | 745 | 940 | 1800 |

table continued on next page

TABLE 3.4 (continued)

| Number | $A_2^c$ degrees C | $A_3^c$ degrees C | s degrees C per second |
|---|---|---|---|
| 19 | 750 | 898 | 3570 |
| 20 | 760 | 933 | 3850 |
| 21 | 760 | 940 | 6300 |
| 22 | 765 | 945 | 6300 |
| 23 | 760 | 960 | 7450 |
| 24 | 760 | 945 | 8200 |
| 25 | 745 | 938 | 12000 |
| 26 | 730 | 898 | 14600 |
| 27 | 770 | 958 | 14600 |

MATERIAL: Annealed Armco iron.

## TABLE 3.5

| Number | $A_3^c$ * degrees C | s degrees C per second | $\tau$ seconds |
|---|---|---|---|
| 1 | 905 | 490 | .036 |
| 2 | 905 | 760 | .021 |
| 3 | 910 | 760 | .021 |
| 4 | 920 | 1280 | .018 |
| 5 | 925 | 1670 | .011 |
| 6 | 915 | 1730 | .010 |
| 7 | 935 | 2340 | .0090 |
| 8 | 930 | 2700 | .0060 |
| 9 | 940 | 3140 | .0052 |
| 10 | 935 | 3300 | .0052 |
| 11 | 930 | 4250 | .0044 |
| 12 | 935 | 5700 | .0040 |
| 13 | 940 | 6000 | .0040 |
| 14 | 945 | 6050 | .0025 |
| 15 | 945 | 6300 | .0025 |
| 16 | 965 | 9650 | .0013 |
| 17 | 960 | 9700 | .0018 |
| 18 | 955 | 9900 | .0025 |
| 19 | 950 | 10600 | - |
| 20 | 960 | 10800 | .0016 |

MATERIAL: Armco iron, as received.

* corrected values; see section 5.3 of the appendix.

## TABLE 3.6

| Number | $A_3^c$ * degrees C | s degrees C per second |
|---|---|---|
| 1 | 905 | 375 |
| 2 | 910 | 640 |
| 3 | 910 | 1090 |
| 4 | 925 | 1530 |
| 5 | 920 | 2270 |
| 6 | 935 | 3300 |
| 7 | 933 | 4200 |
| 8 | 930 | 5200 |
| 9 | 940 | 6300 |
| 10 | 933 | 7400 |
| 11 | 935 | 7500 |
| 12 | 940 | 7900 |
| 13 | 945 | 9600 |
| 14 | 930 | 10500 |

MATERIAL: Annealed Armco iron.

* corrected values; see section 5.3 of the appendix.

# TABLE 3.7

| | | |
|---|---|---|
| Key: | $T_1$ | lower transformation temperature. |
| | $T_2$ | upper transformation temperature. |
| | $s^1$ | heating rate at 720°C. |

Please refer to section 5.2 of the appendix for further explanation of these terms.

| Number | $T_1$ | $T_2$ | $s^1$ | $\log_{10}(s^1)$ |
|---|---|---|---|---|
| 1 | 725 | 750 | 480 | 2.68 |
| 2 | 735 | 765 | 550 | 2.74 |
| 3 | 745 | 780 | 1400 | 3.15 |
| 4 | 730 | 795 | 2000 | 3.30 |
| 5 | 770 | 820 | 3200 | 3.51 |
| 6 | 790 | 840 | 4200 | 3.62 |
| 7 | 770 | 820 | 4600 | 3.66 |
| 8 | 810 | 875 | 6300 | 3.80 |
| 9 | 770 | 835 | 7000 | 3.85 |
| 10 | 815 | 870 | 8600 | 3.93 |
| 11 | 795 | 870 | 12300 | 4.09 |
| 12 | 840 | 890 | 14000 | 4.15 |
| 13 | 830 | 910 | 16800 | 4.23 |
| 14 | 805 | 880 | 19300 | 4.29 |
| 15 | | 960 | 27600 | 4.44 |
| 16 | 840 | 965 | 32300 | 4.51 |

MATERIAL: Annealed hypereutectoid steel.

## TABLE 3.8

Radiative Heating Results.

| Heating rate, degrees C per second: | 330 | 375 | 390 | 400 | 420 | 675 | 1125 |
|---|---|---|---|---|---|---|---|
| $A_3^c$, degrees C: | 915 | 905 | 905 | 920 | 900 | 940 | 925 |

The material used was iron supplied by Johnson, Matthey and Mallory and Company, of Toronto, containing 0.03 per cent carbon and less than 10 parts per million of any metallic impurity.

# 4. DISCUSSION

## 4.1 The Temperature Measurement Technique.

Section 2.7 described several precautions taken to check the accuracy of the temperature-measurement technique. The results were as follows:

(1) No systematic difference was observed between the results of experiments performed in air and of those performed under a protective helium atmosphere, in spite of the appearance of a dark layer of oxide on the surface of specimens of the former series after the heating cycle. (Experiments in which the specimen was held at 800°C were conducted in the helium atmosphere only.)

(2) Reversal of the thermocouple order revealed a systematic difference in results only if the specimen was held at 800°C before applying the final heating pulse. The magnitude of the difference is about 10°C at the most (figures 3.5 and 3.6), and it is presumably due to the fact that a severe thermal gradient was set up along each specimen during the holding period. The true transformation temperature - if no other errors are involved - must therefore lie on the curves shown in figure 3.5 and figure 3.6.

(3) The use of "dummy" alumel-alumel-alumel or chromel-chromel-

chromel leads revealed the existence of a small and apparently random error, which may have been caused by unequal spacing of the thermocouple leads along the specimen or by the presence of a thermal gradient along the specimen at high temperatures. The error involved was indicated by the deviation of the oscilloscope trace from the horizontal during the heating cycle, and was occasionally as large as plus or minus 800 microvolts (corresponding to plus or minus 20°C at 900°C). It seems likely that this was the major source of the scatter of experimental results apparent in each of figures 3.1 to 3.7. However, the possibility of a compositional variation occurring from one specimen to another cannot be ignored, and such variation would also contribute to the observed scatter.

(4) The small number of results obtained by the use of platinum versus platinum-ten per cent rhodium thermocouples fell at random within the limits of scatter for those from the main series of experiments.

(5) Etching or polishing the cold-worked specimens before attaching the thermocouples had no systematic effect on the results.

## 4.2 Treatment of Data.

It seems reasonable to conclude from the foregoing section that the

possibility of systematic errors can be neglected, except for those which may be inherent in the use of the oscilloscope and chart recorder to measure time and voltage. The manufacturer's specifications are as follows:

| | | | | |
|---|---|---|---|---|
| Oscilloscope: | Time base | ± 3 per cent. | Voltage | ± 3 per cent |
| Chart Recorder: | Chart speed | ± 5 per cent. | Voltage | ± ½ per cent |

Calibration of these instruments against a Leeds and Northrup potentiometer, however, showed that the voltage error is probably less than one per cent of the full scale reading on the voltage scales used in this investigation. The corresponding systematic error in temperature is less than 10°C.

The appearance of the results presented in figures 3.1 to 3.4 suggested the application of linear regression analysis to the observations on rates above 200°C per second, in each case, and the curves drawn are the results of such analysis. The results for rates below 200°C per second in figures 3.3 and 3.4 were not rigorously analysed, and the lines shown are only approximate "best-fit" curves through the experimental points; this qualification also applies to all results presented in figures 3.5 to 3.9.

Estimates of the errors involved in reading the values of the various parameters from the heating curves (see section 5.2 of the appendix) are tabulated below:

TABLE 4.1

| FIGURE | PARAMETER | OSCILLOGRAM | CHART |
|---|---|---|---|
| 3.1 to 3.4 | $A_2^c$ | ± 0.4 m.v. (10°C) | ± 0.2 m.v. (5°C) |
| | $A_3^c$ | ± 0.4 m.v. (10°C) | ± 0.2 m.v. (5°C |
| | s | ± 2 pct. | ± 1 pct. |
| 3.5, 3.6 | $A_3^c$ | ± 0.2 m.v. (5°C) | - |
| | s | ± 2 pct. | - |
| 3.7 | $T_1$ | ± 0.4 m.v. (10°C) | - |
| | $T_2$ | ± 0.4 m.v. (10°C) | - |
| | s | ± 5 pct. | - |
| 3.8, 3.9 | $\tau$ | ± 10 pct. | - |
| | s | ± 2 pct. | - |

It is clear that these errors are insufficiently large to account for the scatter of many of the observed results about the "best-fit" lines; the point has been discussed in section 4.1, above.

## 4.3 Interpretation of Results.

### 4.3.1 Introduction.

The most significant result emerging from this investigation is that when Armco iron is heated rapidly from room temperature,

the $A_3^c$ temperature is very nearly independent of the heating rate (figures 3.1 to 3.4). Analogous behaviour on cooling - that is, constancy of transformation temperature over a range of cooling rates - is generally accepted as a criterion for a martensitic or "diffusionless" transformation.

It appears from the results of Boedtker and Duwez (1962), that the $A_3^c$ temperature of rapidly-heated iron, containing about seventy parts per million carbon, is rate-dependent, the transformation being delayed by carbon diffusion. Work on Armco iron at relatively low heating rates, however, has produced results in excellent agreement with those of the present investigation (Svechnikov et al, 1959). In rationalizing the discrepancy between these reports, the interaction of the following two factors plays a major part: first, impurities (including carbon) in the iron, and second, the holding temperature prior to rapid heating.

### 4.3.2. The effect of impurities on $A_3^c$.

#### (a) Copper.

Armco iron contains about 0.1 per cent copper - 0.07 per cent in the present case - whereas the iron used by Boedtker and Duwez contained less than one part per million. It is conceivable that if the copper existed as a separate face-centred cubic phase within ferrite at room temperature, this phase might be retained on heating rapidly to the $A_3^c$

temperature, and nucleate the body-centred cubic to face-centred cubic transformation in the iron. There are two objections to this hypothesis: first, although the solubility of copper in alphairon at room temperature is not known, the solubility is at least 0.3 per cent at 700°C, and may be considerably higher (Hansen 1958, Hornbogen and Glenn 1960); second, experiments employing radiative heating of iron containing virtually no copper revealed no significant change in the $A_3^c$ temperature for a heating-rate range of about 250 - 1200°C per second (see table 3.8).

### (b) Oxygen.

The iron used in the present investigation contained more than 0.1 per cent oxygen (table 2.1). However, it is probable that the major part of the oxygen was confined to the surface layers of the iron, making this figure misleading as an indication of the amount of oxygen distributed throughout the iron. Furthermore, the presence of oxygen in concentrations up to about 20 per cent, as a binary constituent, has no effect on the equilibrium $A_3^c$ temperature.

### (c) Nitrogen.

It seems reasonable to assume that the very low concentration of nitrogen (0.0045 per cent) in the iron would make the effect of this element negligible compared to that of carbon (about 0.03 per cent).

### (d) Other impurities, except carbon.

Inspection of the relevant binary phase diagrams (Hansen, 1958) shows that none of the remaining impurities (table 2.1) can be expected to affect the equilibrium $A_3^c$ temperature in the amounts present; there is no reason to suppose that their influence would increase at rapid heating rates.

### (e) Carbon.

The iron-carbon phase diagram for small carbon concentrations is shown in figure 4.1; tentative paths for the rapid heating experiments are superimposed (lines $P_1$ to $P_4$) and holding temperatures are indicated by small circles. It is apparent from this diagram that if iron and cementite are in thermodynamic equilibrium at room temperature, the ferrite contains virtually no carbon in solid solution. Smith reported that in iron containing 0.015 per cent carbon and cooled from 700°C in about thirty minutes, dendritic carbide particles are observed in the ferrite matrix under the electron-microscope (E. Smith, 1960). Other investigations (E. Smith, 1962; see also Smith's reference to work by Sewell) have shown that the growth of carbide particles in quenched iron is complete after aging for a few hours at 200°C. Annealed specimens in the present investigation were cooled from 600°C to room temperature over a period of ten hours or more; it is therefore assumed that the carbon is present as cementite at room temperature. The heat-treatment

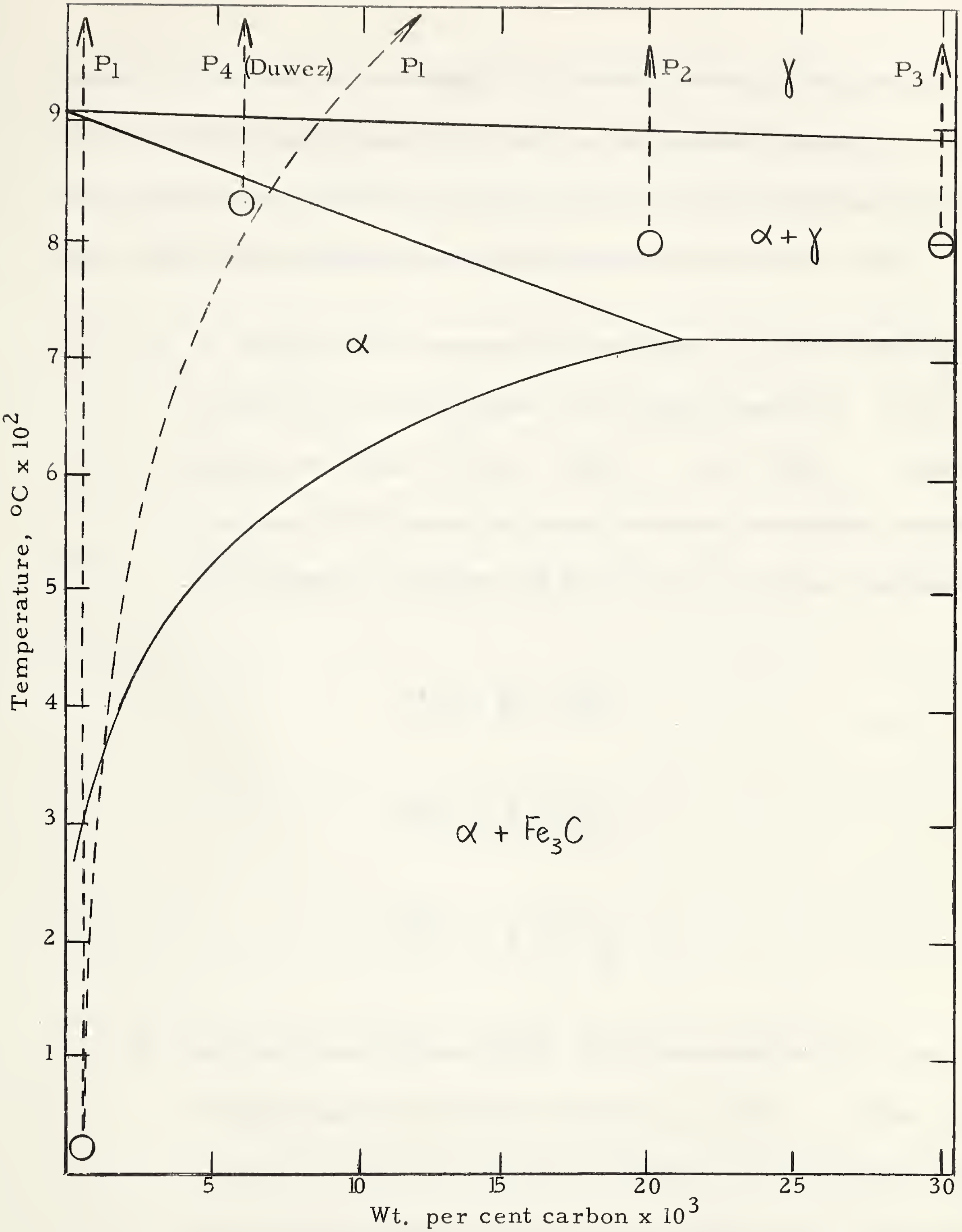

Figure 4.1 Part of the iron-carbon phase diagram (after Hansen).

history of the iron "as-received" is unknown, so the assumption may not be valid for specimens which were not subsequently annealed. If the premise is accepted for annealed specimens, the following considerations show that a diffusionless transformation may occur at $A_3^c$:

(1) E. Smith (1962) reported that cementite, in iron containing about 0.02 per cent carbon, lies predominantly on $\{110\}_\alpha$ planes and along $\langle 111\rangle_\alpha$ , $\langle 110\rangle_\alpha$ and $\langle 112\rangle_\alpha$ directions. Andrews (1963) listed the most persistent orientation relationship between cementite and ferrite under various conditions as

$$(001)_c \parallel (112)_\alpha$$

$$[100]_c \parallel [110]_\alpha$$

$$[010]_c \parallel [111]_\alpha$$

(2) Agarwala and Wilman (1953, 1954) proposed that the $\alpha \rightarrow \gamma$ transformation occurred by shear on $\{211\}_\alpha$ along $\langle 111\rangle_\alpha$, leaving $\{110\}_\alpha$ as the phase interface. Burgers and Bogers (1964) have pointed out that a body-centred cubic lattice could transform to a face-centred cubic one by shear along $\{110\}_\alpha$, $\langle 110\rangle_\alpha$ followed by shear along $\{110\}_\alpha \langle 112\rangle_\alpha$ (see also Cohen

et al., 1961). Since a unit dislocation along $\langle 111 \rangle_{\alpha}$ can dissociate into two partial dislocations along $\langle 110 \rangle_{\alpha}$ and $\langle 112 \rangle_{\alpha}$ it is clear that the two mechanisms are closely related.

It might be concluded from the foregoing evidence that, on rapid heating, the $\alpha \rightarrow \gamma$ transformation occurs by a shear mechanism, triggered off by the lattice strain imposed by cementite plates lying in precisely those orientations necessary to describe the shear. Such a mechanism would account for the fact that the $A_3^c$ temperature is very nearly independent of heating-rate at the faster rates, and it is allied to the mechanism proposed by Kidin (1957) for the transformation at $A_3^c$ in mild steel (see also section 1.3). The small elevation of $A_3^c$ temperature that occurs at lower heating rates could then be explained as an effect of diffusion-control of the transformation.* The fact that it is more pronounced for specimens annealed at a higher temperature (compare figures 3.3 and 3.4) suggests that nucleation is occurring at the grain-boundaries. It is interesting to note that the upper curve in the figure 3.4 can be described by the Arrhenius-type equation

$$T = a \exp \left\{ -b \, (\text{rate}) \right\}$$

---

* Compare the behaviour of $A_3^c$ on rapid cooling (Bibby and Parr, 1964).

(where a and b are constants) although insufficient data have been obtained to develop this quantitatively.

Thus the hypothesis calls for a diffusion-controlled process for rates up to about 200°C per second (for the largest grain-size; lower critical rates for smaller grain-sizes), and a process that is largely diffusionless ("massive" or martensitic) for higher rates. A useful way of looking at this is in terms of the average diffusion-length, for iron atoms in the time available for transformation (see figure 4.2). Progressively faster rates push the Gaussian distribution (3) of diffusion lengths for a diffusion-controlled process towards $|\lambda|_0$, the ultimate stage of a "pure" martensitic (diffusionless) transformation being represented by the delta-function (1) whilst the "massive" transformation, characterized by very short-range diffusion, is intermediate (2).

Thus the diffusionless transformation seems to offer a plausible mechanism in the present case; there is, however, a number of further arguments to consider.

### 4.3.3. Diffusion rates.

If the diffusion process is to be suppressed in the interval between the equilibrium $A_3^c$ temperature (910°C for pure iron, a little lower for Armco iron) and the observed $A_3^c$, it is reasonable to assume that the diffusion length must be reduced to the same order of magnitude as the

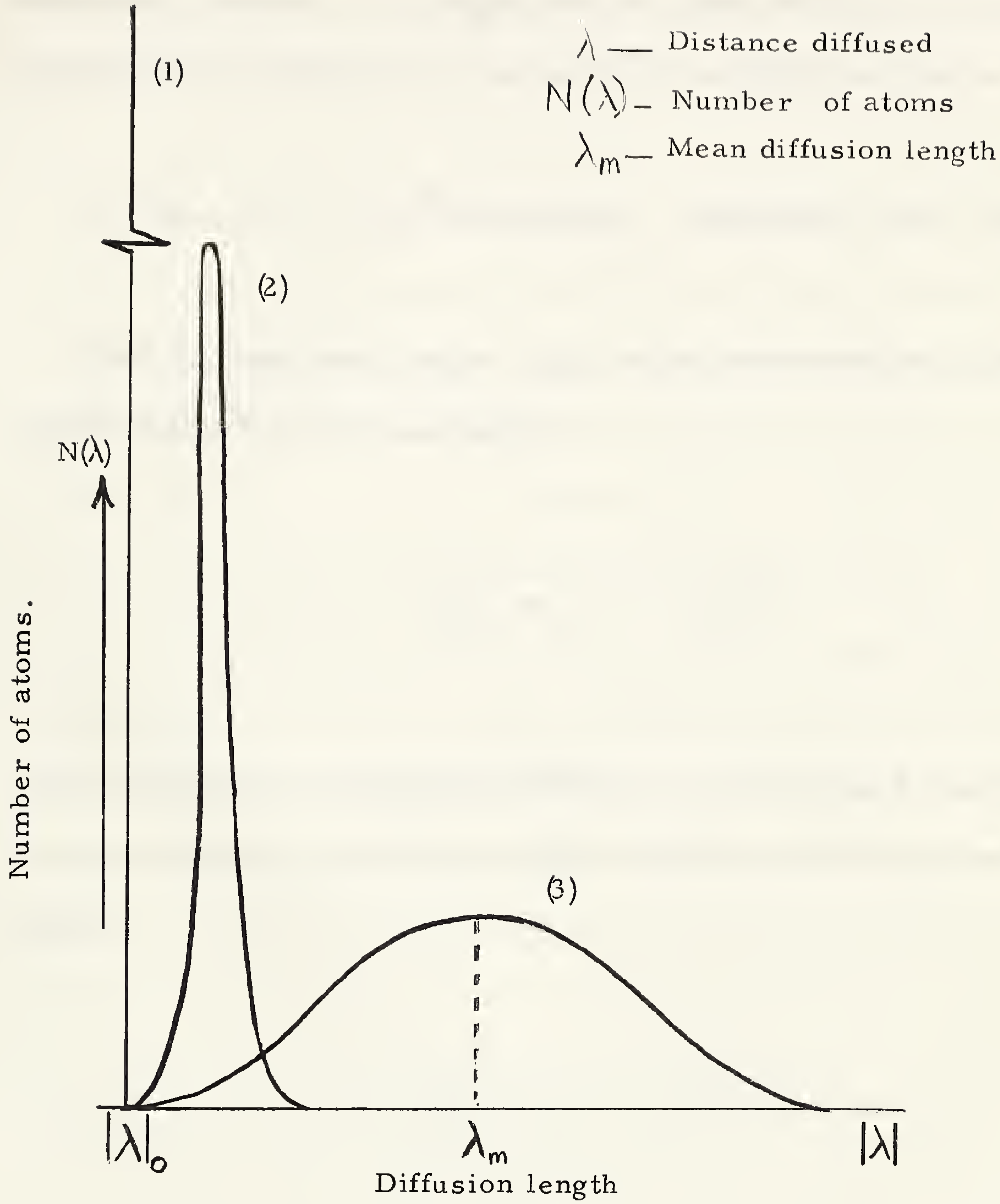

Figure 4.2 Classification of phase transformations by diffusion lengths.

interatomic distance, at a heating rate of about 200°C per second. The self-diffusion coefficient for iron in ferrite at 905°C is given by

$$D \doteqdot 5 \times 10^{-11} \text{ cm.}^2 \text{ per second} \qquad \text{(Buffington et al., 1961)}$$

Now the mean path length, $\lambda_m$, can be determined to a first approximation from the expression

$$\lambda_m \doteqdot \sqrt{Dt}$$

where t is the time available for diffusion - in this case 0.1 second, as the temperature is raised from 905°C to 925°C at 200°C per second. Hence,

$$\lambda_m \doteqdot 2 \times 10^{-6} \text{ cms.}$$

which is two orders of magnitude too large for the delta-function limit of diffusion length, the interatomic distance being approximately $3 \times 10^{-8}$ cms. However, self-diffusion of iron proceeds by a vacancy mechanism, and at fast enough heating rates one might expect the

relaxation time, $\tau_v$, for the establishment of the equilibrium number of vacancies at about 905°C to become significant: if t and $\tau_v$ were of the same order of magnitude, the effective value of $\lambda_m$ would be considerably smaller. Unfortunately, it is difficult to estimate the effective value of $\lambda_m$ for a given heating-rate, since $\tau_v$ has not been determined.

It may also be possible for an appreciable amount of carbon to diffuse from the cementite into the alpha matrix between about 500°C and the observed $A_3^c$ temperature, at heating rates as high as 200°C per second.* Results already referred to (Boedtker and Duwez, 1962) show that for a carbon concentration of 0.007 per cent, homogeneously distributed throughout the ferrite, the activation energy for carbon diffusion may be an important factor in deciding the $A_3^c$ temperature. It seems necessary, however, to assume that in the present investigation the carbon was mostly retained as cementite until the $A_3^c$ temperature was reached (as indicated by the dashed curve in figure 4.1), if the delay-times observed by Boedtker and Duwez are indeed due to the effect of interstitial carbon atoms as they suggest. The fact that carbon segregation to vacancies at very low carbon concentration is thought to inhibit diffusion

---

* A comparison of diffusivities for self-diffusion ($D \doteqdot 5 \times 10^{-11}$ cm.$^2$ per second at 900°C - Buffington et al., 1961) and carbon diffusion ($D \doteqdot 10^{-6}$ cm.$^2$ per second at 900°C - R. P. Smith, 1962) in alpha iron, indicates that the average diffusion length of the carbon atoms is several orders of magnitude higher than that of the iron atoms.

mechanisms(in this case producing a carbon-saturated region immediately around the cementite particles) is further evidence in support of the diffusionless transformation hypothesis.

The effect of a more homogeneous carbon distribution was investigated by heating a number of specimens from 800$^{o}$C (in the $\alpha + \gamma$ region) instead of from room temperature; the $A_{\xi}$ temperature exhibited continuous elevation with increasing rate in spite of the presence of $\gamma$ nuclei before the application of the final heating pulse (figures 3.5, 3.6, 4.1). This behaviour is compatible with the idea that carbon diffusion is now rate-controlling, the cementite no longer being present to trigger a diffusionless process; the curves can again be described by an Arrhenius-type equation. The elevation of the transformation temperature in hypo-eutectoid steel (figure 3.7) can be explained in a similar way by considering the diffusion of carbon in cementite as the rate-controlling factor.* It is interesting to note in this context that the shape of the $A_{\xi}$ versus rate curve for iron, held at 800$^{o}$C before heating, is very similar to the transformation temperature versus rate curve for the steel.

### 4.3.4 The transformation time.

The inverse dependence of transformation time on heating-rate for

---

* by diffusional growth of $\gamma$ nuclei formed at the cementite-ferrite interface.

the cold-worked iron (figures 3.8, 3.9) indicates that a critical (and constant) amount of heat is required to bring the transformation to completion. It was not possible to obtain comparable data for previously annealed specimens since these did not produce a distinctly horizontal thermal arrest in the heating curve on transformation; the phase change in this case was indicated by a more gradual inflexion in the curve, extending over a range of temperature.* (A mean value was taken as the $A_3^c$ temperature.) The following conclusions are tentatively advanced:

(1) Different transformation mechanisms are operative in the cold-worked and annealed specimens.

(2) These are:

  (a) Kidin's "mosaic block" mechanism in the case of the cold-worked specimens, which can be expected to contain sub-grains, and

  (b) the "cementite-nucleated" mecnanism, described above, in the case of the annealed specimens.

The fact that holding at 800°C makes little difference to the calculated latent heat of transformation of previously cold-worked specimens implies either

---

* That the length of the thermal arrest is indicative of the transformation time has been shown by previous investigators (Svechnikov et al., 1955), and their conclusions are supported by the latent heat data obtained in the present work - see part 3.3 of the results section.

(a) that there is no difference in the mechanism of transformation before and after recrystallization,

or (b) that the change in the free energy is the same for the $\alpha \rightarrow \gamma$ transformation whether it proceeds by shear or by diffusion.

The latent heat values obtained from figures 3.8 and 3.9 are in good agreement with those determined by Anderson and Hultgren (1962) for the $\alpha \rightarrow \gamma$ transformation in pure iron, namely, 225 calories per gram molecule plus or minus 15. It is reassuring to note that this is conclusive evidence that the $\alpha \rightarrow \gamma$ transformation is, in fact, occurring.

### 4.3.5 Crystallography.

It is tempting to cite the crystallographic coincidence of cementite orientation and shear propagation directions, described above, as strong evidence that a diffusionless transformation does indeed occur on rapid heating. However, the low indices of the planes and directions reduce the significance of the observation. Solute precipitation and shear are phenomena that almost invariably occur on close-packed planes and in close-packed directions of the crystal lattice; a causal relationship between the two is by no means inevitable.

### 4.3.6 The Curie temperature.

Figures 3.1 to 3.4 reveal, without exception, the constancy of Curie

temperature with respect to heating rate. This result is to be expected in view of the electronic nature of the transition from ferromagnetic to paramagnetic iron (see, for example, Zener, 1955) and provides a further verification of the reliability of the temperature-measurement technique.

## 4.4 Conclusions.

(1) When previously annealed or cold-worked Armco iron is heated rapidly from room temperature, the $A_3^c$ temperature is very nearly independent of the heating-rate.

(2) The behaviour of the $A_3^c$ temperature indicates that the growth of austenite nuclei no longer involves long-range diffusion at heating-rates higher than about 200°C per second; however, the distribution of carbon in the iron is probably of critical importance in deciding the mechanism of transformation.

(3) The time elapsed during the $\alpha \longrightarrow \gamma$ transformation in previously cold-worked material is inversely proportional to the heating-rate. Calculation of the latent heat of transformation gives results in good agreement with those of previous investigations.

(4) The Curie temperature is independent of heating-rate in the range investigated.

# 5. APPENDIX

## 5.1 Shear Model for the $\alpha \rightarrow \gamma$ Transformation in Iron.

Agarwala and Wilman's model is shown schematically in figures 5.1(a) and 5.1(b), as a projection on the $(01\bar{1})_\alpha$ plane. The net atomic movement is along $\langle 111 \rangle_\alpha$ directions (becoming $\langle 110 \rangle_\gamma$) as in normal translational slip in the respective lattices, and in this way a $\sqrt{2}$-rectangular array in the $(01\bar{1})_\alpha$ plane becomes a square array in $(001)_\gamma$. (Agarwala and Wilman, 1953, 1954.)

## 5.2 Measurement of Parameters from the Heating Curve.

A typical heating curve from one of the oscillograms has been drawn schematically in figure 5.2 (not to scale). The following parameters were measured directly:

(i) $s$ slope of line A'B' (AB produced).

(ii) $\tau$ time elapsed during transformation.

(iii) $e_1$ e.m.f. between Curie point and base-line (room temperature).

(iv) $e_2$ e.m.f. between transformation start temperature and base-line.

(v) $e_3$ e.m.f. between transformation finish temperature and base-line.

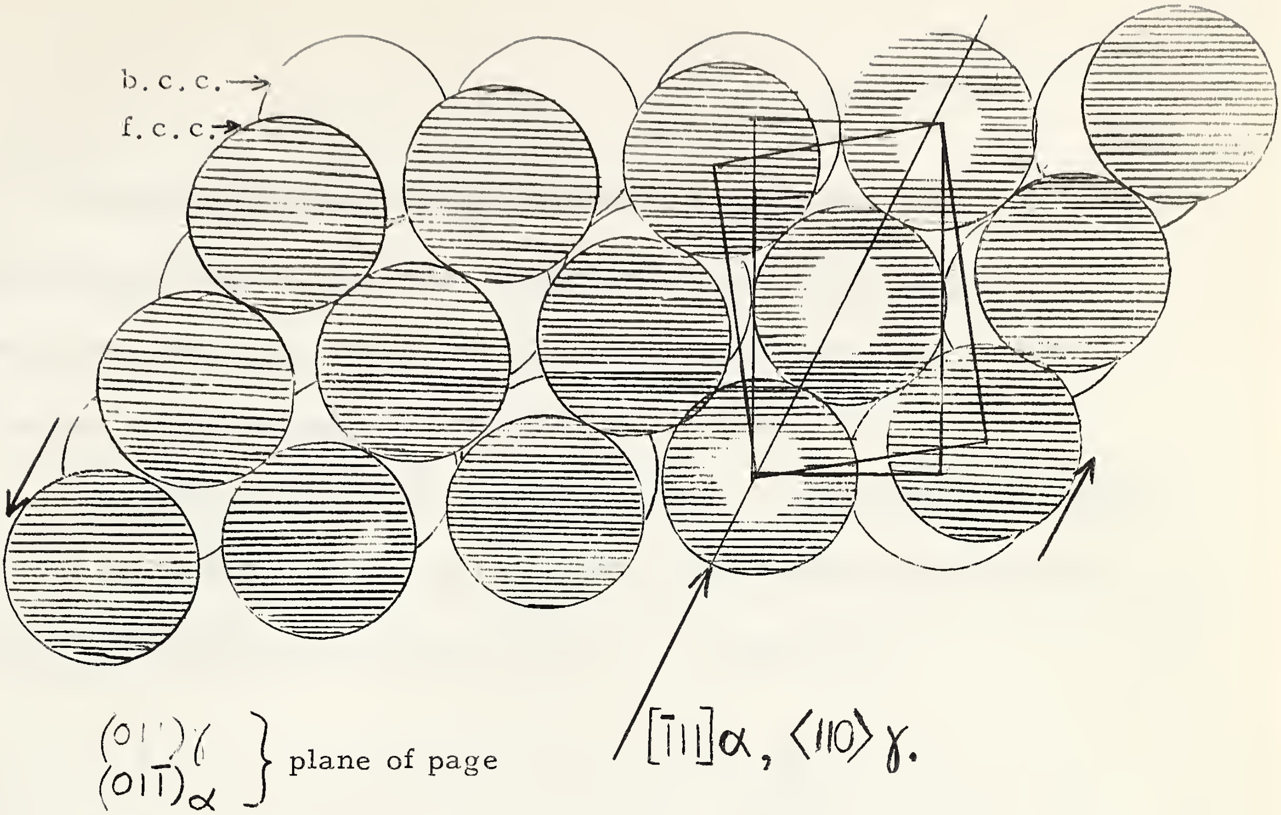

Figure 5.1 (a) Shear model for the $\alpha \rightarrow \gamma$ transformation, single plane.

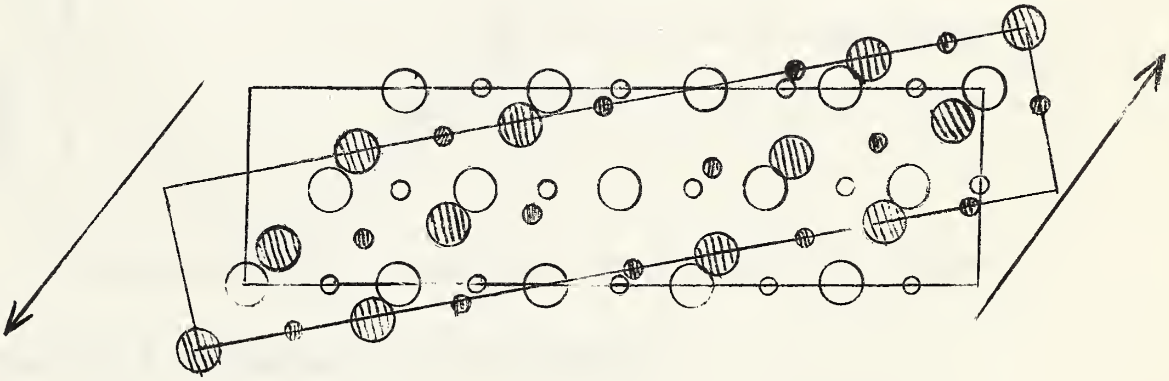

O, o at heights ± 0, 1, 2, 3 . . . . $\times \sqrt{2}\, a_\alpha$ and $\pm \frac{1}{2}, \frac{3}{2}, \frac{5}{2}, \dots \times \sqrt{2}\, a_\alpha$, respectively.

⊘, ⊘ at heights ± 0, 1, 2, 3 . . . . $\times C_\gamma$, $\pm \frac{1}{2}, \frac{3}{2}, \frac{5}{2}, \dots \times C_\gamma$, respectively.

Figure 5.1 (b) Shear model for the $\alpha \rightarrow \gamma$ transformation, (after Agarwala and Wilman).

The appropriate temperatures were then calculated using standard thermocouple tables; the mean heating rate from the Curie point to the transformation temperature was calculated by converting s from millivolts per second to degrees Centigrade per second.

The transformation temperature was taken as the mean value corresponding to the e.m.f. $(e_2 + e_3)/2$. For cold-worked specimens the thermal arrest was horizontal, so that: $e_2 = e_3$ .

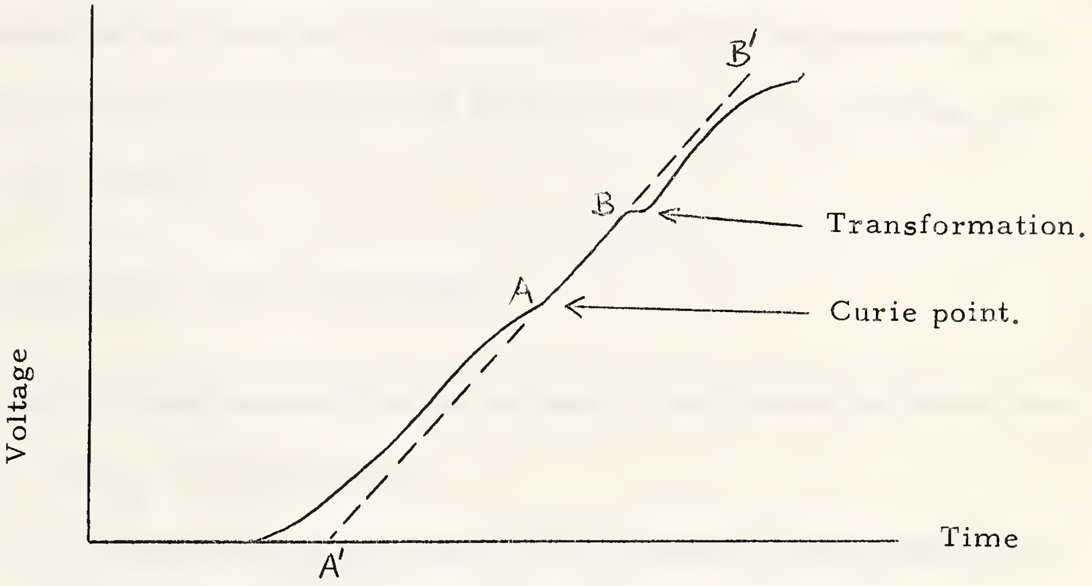

Figure 5.2 Heating-curve parameters.

The heating rate for those iron specimens held at 800°C prior to final heating was taken as the mean rate between 800°C and $A_3^c$. Measurement of the heating rate for steel specimens was accomplished by calculating the slope of the tangent to the heating curve at 720°C; two distinct "kinks" were observed in these curves, and the mean temperature of each was plotted accordingly. (Table 3.7, $T_1$ and $T_2$; see also figure 3.7.)

## 5.3 Correction of the Transformation Temperature.

Holding a specimen for one minute at 800°C caused a steady thermal gradient to be set up along its length due to heat losses to the brass terminals. This effect upset the e.m.f. balance which had been established at room temperature to nullify nonthermal contributions, and produced in turn a discontinuity in the indicated temperature on closing the main power switch for rapid heating. The ensuing error was eliminated by combining the observed $A_3^c$ temperature with the temperature gap corresponding to the height of the discontinuity; thus a corrected $A_3^c$ value was obtained.

## 5.4 Calculation of the Latent Heat.

The following assumptions were made in calculating the latent heat of the $\alpha \rightarrow \gamma$ transformation:

(i) That the rate of heat input to the specimen is the same during the transformation and immediately before it.

(ii) That the rate of heat loss to the surroundings is the same during the transformation and immediately before it.

In the notation of section 5.2, the rate of heat input per gram of iron, W, for each degree rise in temperature is given by:

$$W = Cs$$

where C is the specific heat of alpha iron just before the transformation.

During the transformation,

$$W = \frac{L}{\tau}$$

Hence,

$$L = Cs\tau$$

Thus by taking an average value for C in that range 850°C to 910°C, *

L was determined from the experimental values of s and $\tau$ .

---

* $C \doteq 9.5$ calories per gram-atom. (Anderson and Hultgren, 1962.)

# BIBLIOGRAPHY

Agarwala, R. P., and H. Wilman, Proc. Phys. Soc. 1953, 66B, 717-719.
idem, Proc. Roy. Soc. 1954, 223A, 167-174.

Anderson, P. D., and R. Hultgren, Trans. A. I. M. E. 1962, 224, 842-845.

Andrews, K. W., Acta Met. 1964, 12, 255-261.

Bibby, M. J., and J. Gordon Parr, J. I. S. I. 1964, 202, 100-104.

Bodyako, M. N., Yu. M. Loiko, B. L. Pavlyukevich and V. I. Parkhimovich, Metalloved. Term. Obra. Met. 1960, 1, 49-52.

Boedtker, O. A., and P. Duwez, Report No. 3 to O. N. R., C. I. T. (Pasadena) March 1962.

Bogers, A. J., and W. G. Burgers, Acta Met. 1964, 12, 255-261.

Buerger, M. J., "Phase Transformations in Solids", Wiley, New York 1951.

Buffington, F. S., K. Hirano and M. Cohen, Acta Met. 1961, 9, 434-439.

Cohen, J. B., R. Hinton, K. Lay and S. Sass, ibid. 894-895.

Hansen, M., "Constitution of Binary Alloys", McGraw-Hill, New York 1958.

Hornbogen, E., and R. C. Glenn, Trans. A. I. M. E. 1960, 218, 1064-1070.

Kidin, I. N., "Phase Transformations in Steel on Rapid Heating", Metallurgizdat, Moscow 1957.
idem, Izvest. VUZ Chern. Met. 1960, 1, 142-146 (No. 1)
idem, Proiz. Obra. Stal. 1960, 33, 250-266 (No. 2)

Kuznetsov, B. A., Metallov. Obra. Met. 1958, 2, 28-35.

## BIBLIOGRAPHY (continued)

Mehl, R. F., "Brief History of the Science of Metals", A. I. M. E., Chicago 1948.

Parr, J. Gordon, Sorby Centennial Meeting 1963, (to be published).

Radcliffe, S. V., L. Kaufman and M. Cohen, Acta Met. 1962, 10, 1110-1111.

Seitz, F., "The Modern Theory of Solids", McGraw-Hill, New York 1940, 487-488.

Singh, K. P., and J. Gordon Parr, Acta Met. 1962, 10, 1111-1112.

Smith, C. S., "A History of Metallography", University of Chicago Press, 1960.

Smith, E., Acta Met. 1960, 8, 403-404.
idem, in "Direct Observation of Imperfections in Crystals", Interscience, New York 1962, 203-211.

Smith, R. P., Trans. A. I. M. E. 1962, 224, 105-111.

Smoluchowski, R., and J. S. Koehler, Ann. Rev. Phys. Chem. 1941, 2, 241.

Sorby, H. C., J. I. S. I. 1887, (ii), 264.

Svechnikov, V. N., V. I. Gridnev and Yu. A. Kocherzhinsky, Dok. Akad. Nauk. U. S. S. R. 1955, 103, No. 6, 1025-1026.

Svechnikov, V. N., and Yu. A. Kocherzhinsky, Voprosy Fiz. Met. Metall. 1959, 10, 182-185.

Zener, C., A. I. M. E. Journal of Metals 1955, 7, 619-630.

B29816